Nonidet P-40 all in isopropanol) was added. The plate was covered with aluminum foil, and the cells were agitated on an orbital shaker for 15 min, after which time the absorbance was read at 590 nm with a reference filter of 620 nm using a Bio-Rad model 680 microplate reader (Bio-Rad, Hercules, CA, USA).

Statistical analysis

The SPSS version 21 software package was used for all statistical analyses. All experimental data were reported as the mean ± SD. Mean values of continuous variables were compared using a two-tailed *t*-test for independent samples. *P*-values of less than 0.05 and 0.01 were considered significant and highly significant, respectively.

RESULTS

Clinical findings

The current panoramic radiographs of the two affected individuals and the pedigree of each patient are shown in Figures 1a, b, d and e. Patient 1 is the first child of her family, and her parents and younger sister is normal. Patient 2 is the second child of her family, and her parents and elder brother is normal. Therefore, both cases are sporadic mutations. In this study, more details of the dental phenotypes of the patients were examined. The record of an oral examination of patient 1 (first visit: 16Y6M) showed nine missing and six impacted teeth, persistent primary teeth, delayed secondary dentition, radiculomegaly, malformed teeth and cleft palate. Patient 2 (first visit: 10Y9M) had similar but less severe oral phenotypes. She had only two missing teeth, one impacted tooth and submucous cleft palate. The details of the dental phenotypes at the initial stage are summarized in the diagrams in Figures 1c and f.

Mutation analysis

Genetic analysis showed that patient 1 harbored a heterozygous intronic polymorphism, c.166-55G>A, and a heterozygous nonsense mutation, c.*4794G>A (p.W1598*). The results of the healthy parents of patient 1 showed that the father and mother harbored the same intronic polymorphism, homozygous in the father and heterozygous in the mother, but not the nonsense mutation (Figures 2a and b). This intronic polymorphism was reported in the Japanese Single Nucleotide Polymorphisms Database, reference as rs6610384. Patient 2 harbored a heterozygous frameshift mutation, c.3668delC (p.S1223Wfs*15), whereas her healthy mother did not have any mutations (Figure 2c). Disease-causing potential analyzed by Mutation Taster showed that the nonsense and frameshift mutations are predicted to cause disease, and no single nucleotide polymorphisms in the altered region were found. These two mutations had not been previously reported. The positions of the mutations and polymorphism relative to the *BCOR* exons and protein are depicted in Figure 2d.

Cell culture and characterization of cultured cells

The first premolar from patient 2 was 39.2 mm in length, approximately two times longer than normal (Figure 3a). As a comparison, the normal tooth length of the lower first premolar is reported to be 22.5 mm.[25] Cultured mutant pulp and PDL cells harvested from patient 2's tooth are pictured in Figures 3b and c. Cellular *BCOR* gene sequences were identical to those from the buccal swab (data not shown). *VIM* was strongly expressed in mutant pulp, but *KRT14* was not, suggesting that most of the cultured mutant pulp cells were mesenchymal and that few were epithelial cells. By contrast, VIM and *KRT14* were both highly expressed in the mutant PDL cells and more highly than in mutant pulp cells. We conclude that cultured mutant PDL cells include both mesenchymal and epithelial cells and could be expected to have more mesenchymal and epithelial characteristics than cultured mutant pulp. The PCR results are shown in Figure 3d.

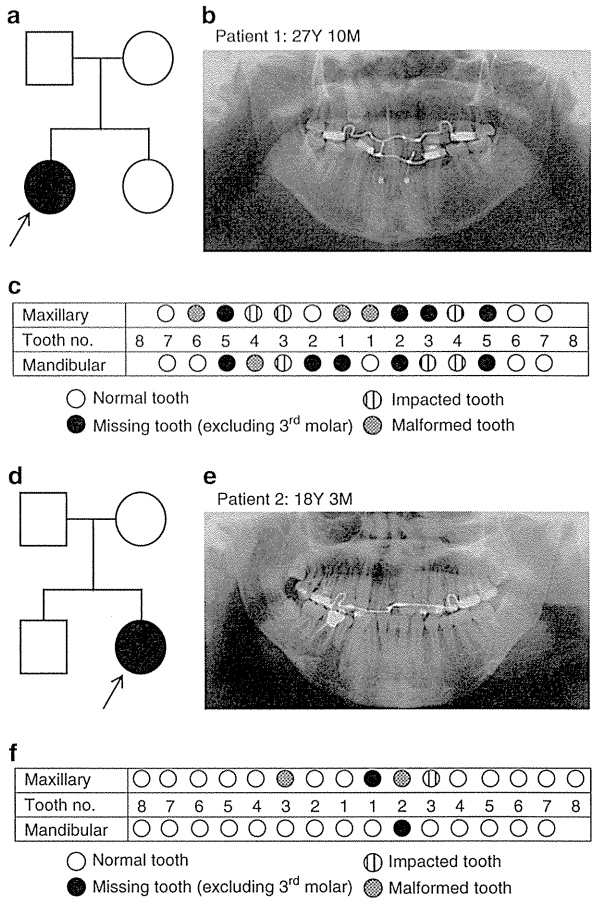

Figure 1 Family pedigree, current panoramic radiograph and summarized dental phenotypes of the two patients. The results of patient 1 are shown in **a–c**, and the results of patient 2 are shown in **d–f**. (**a**) Family pedigree of patient 1. The arrow indicates patient 1. (**b**) Current panoramic radiograph of patient 1 showing remarkably long roots in many teeth, especially in the anterior and premolar region. (**c**) Summary of the dental phenotype at the initial stage of patient 1. (**d**) Family pedigree of patient 2. The arrow indicates patient 2. (**e**) The current panoramic radiograph of patient 2 also shows remarkably long roots and open apices in many teeth in the anterior and premolar region. (**f**) Summary of the dental phenotype at the initial stage of patient 2.

BCOR expression

BCOR expression was detected in pulp and PDL in both wild-type and mutant cultures. *BCOR* expression was significantly higher in PDL cultures than in pulp cultures for both wild-type and mutant cultures. In PDL cultures, *BCOR* expression was significantly lower in mutant than wild-type cultures. The expression did not differ between mutant and wild-type pulp cultures. The results are shown in Figure 3e.

Analysis of NMD

Wild-type and mutant cells derived from both pulp and PDL showed increased *BCOR* transcript levels after the inhibition of translation elongation by the addition of CHX. The differential expression of

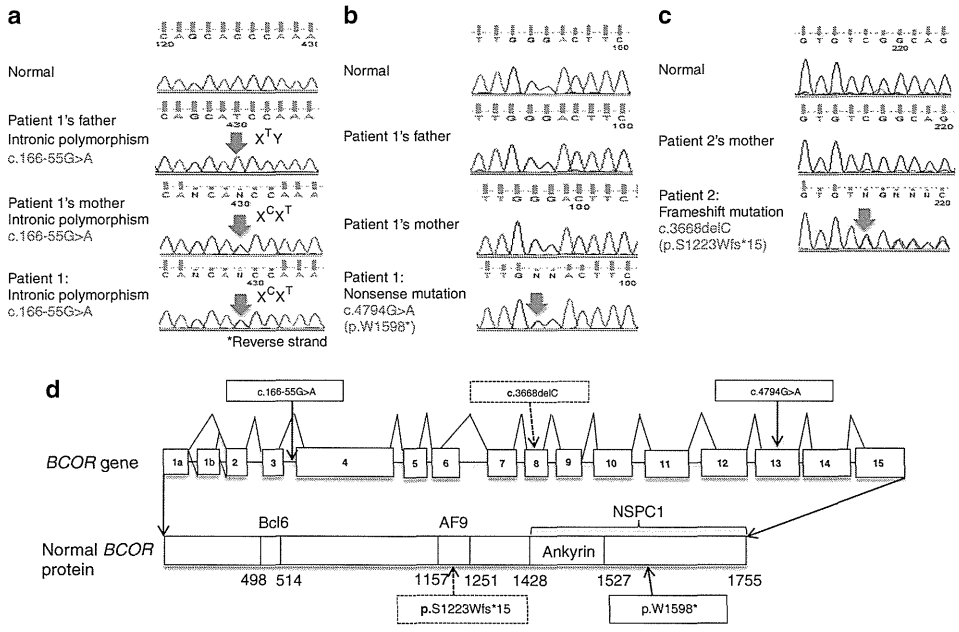

Figure 2 Genetic analysis. (**a** and **b**) Patient 1 had an intronic polymorphism, c.166-55G>A and a nonsense mutation, c.4794G>A, which caused the truncated protein p.W1598*. However, her parents harbored only the intronic polymorphism. (**c**) Patient 2 had a frameshift mutation, c.3668delC, which caused the truncated protein p.S1223Wfs*15, whereas her mother's sequence was normal. (**d**) The positions of the variations in *BCOR* relative to the exons and the protein. The variations in patient 1 are shown as solid-line arrows and boxes. The variation in patient 2 is shown as a dotted-line arrow and box. Bcl6, the region that interacts with Bcl6; AF9, the region that interacts with AF9, the common mixed lineage leukemia gene fusion partner; NSPC1, the region that interacts with nervous system polycomb1; Ankyrin, ankyrin repeats that are involved in protein–protein interactions and protein structure.

BCOR was determined by dividing post-CHX transcript levels by pre-CHX transcript levels. This value reflected the fold change in transcript levels due to the inhibitory effect of CHX (fold induction). The differential expression of *BCOR* did not differ between mutant and normal pulp but was significantly higher in mutant PDL than wild-type PDL, as shown in Figures 3f and g. However, in both cell types, NMD had a partial effect on transcript levels as indicated by the detection of all heterozygous sequences in the cDNA both before and after adding CHX (Figure 3h).

Analysis of RNA stability

Mutant *BCOR* transcripts in the PDL cells of patient 2 degraded within 3 h after the addition of actinomycin D and were more unstable than were those of the wild type. In pulp cells, by contrast, the mutant *BCOR* transcript level was not significantly different from normal. The results are shown in Figures 4a and b.

Cell proliferation rate

The MTT assay showed that the mutant PDL cells proliferated faster than the wild-type cells but that the mutant pulp cell proliferation rate was likely normal, as shown in Figures 4c and d.

DISCUSSION

The two patients were diagnosed with OFCD syndrome based on a distinct pattern of eye, craniofacial, heart and dental anomalies. According to their family pedigrees, their parents and siblings are healthy, so both patients had sporadic mutations. Patient 1 had a heterozygous intronic polymorphism, c.166-55G>A, and a heterozygous nonsense mutation, c.*4794G>A (p.W1598*). The intronic polymorphism was also found in her healthy parents: the homozygous father and heterozygous mother, and among Japanese people as determined by the Japanese Single Nucleotide Polymorphisms Database, reference as rs6610384. The population diversity of this single nucleotide polymorphism showed that Japanese population in Tokyo have allele C = 33.1% and allele T = 66.9% in the reverse stand sequence. Therefore, this single nucleotide polymorphism is non-pathogenic and can be found in normal population. Patient 2 was found to have a heterozygous frameshift mutation, c.3668delC (p.S1223Wfs*15), but her healthy mother did not. Furthermore, disease-causing potential analyzed by Mutation Taster showed that the nonsense and frameshift mutations are predicted to cause disease, and no single nucleotide polymorphisms in the altered region were found. OFCD syndrome is presumed to have lethal effects on affected male. Previous studies showed that all affected individuals are females, with several incidences of mother–daughter transmission.[1,5,26] There is no report of males developing this condition.[4,8] However, the patient 2's father was not included in our experiment, we assumed that he does not have any pathogenic mutations in *BCOR* gene regarding his normal phenotypes. In addition, a single missense change, c.254C>T (p.P85L) in *BCOR* that has been found in patients with MCOPS2 were not found in our patients. Taken together, these data allow us to conclude that the nonsense mutation in patient 1 and the frameshift mutation in patient 2 contributed to OFCD syndrome; both mutations are pathogenic. A variation in phenotype severity was observed, suggesting that further studies are needed to clarify the genotype–phenotype relationship.

To date, a total of 34 mutations in *BCOR* have been found, most of which result in premature termination of the protein with deletion of the carboxy-terminal domain;[3,6,7] therefore, NMD might have an important role in pathogenesis. Interestingly, the efficiency and

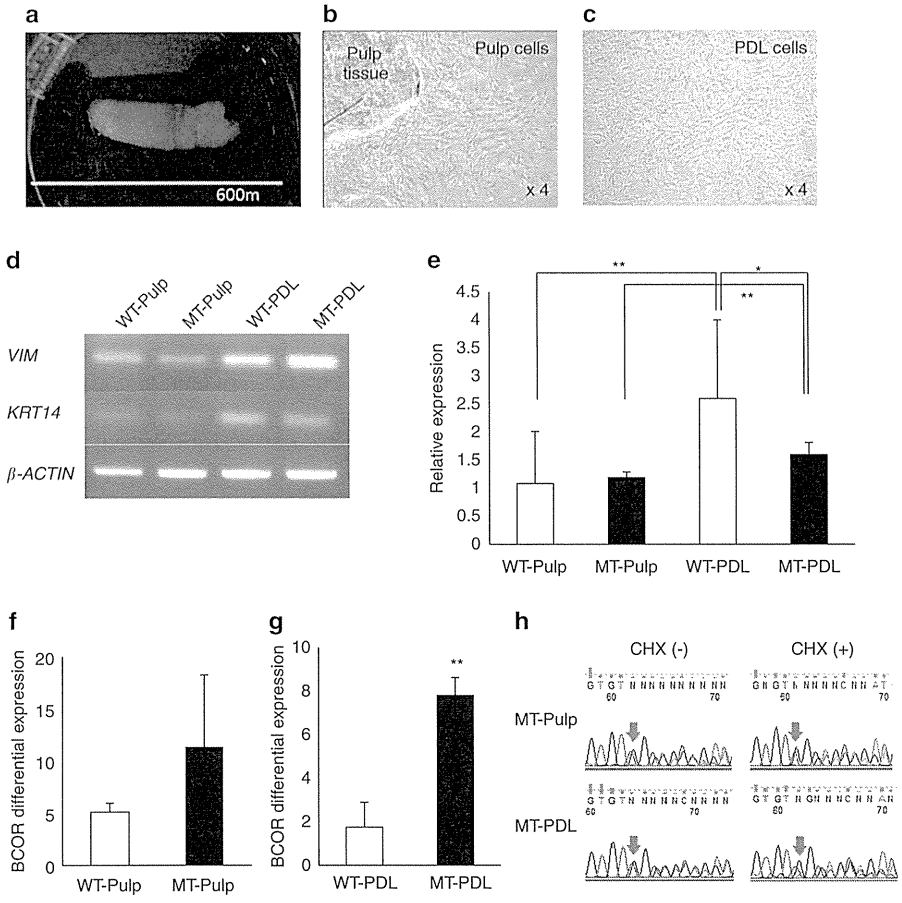

Figure 3 Cultured cells and NMD analysis. (**a**) Lower first premolar of patient 2. It was 39.2 mm in length. (**b** and **c**) Cultured pulp and PDL cells harvested from patient 2's tooth. (**d**) *VIM* and *KRT14* expression in pulp and PDL cells. (**e**) *BCOR* expression in pulp cells and PDL cells. (**f**) *BCOR* differential expression in pulp cells. (**g**) *BCOR* differential expression in PDL cells. (**h**) *BCOR* cDNA sequences of cultured cells before and after adding CHX. WT-Pulp, wild-type pulp; MT-Pulp, mutant pulp; WT-PDL, wild-type PDL; MT-PDL, mutant PDL; CHX(−), before adding CHX; CHX(+), after adding CHX. $^{*}P<0.05$, $^{**}P<0.01$.

sensitivity of the NMD mechanism differ by cell type.[16,17] The effect of NMD on a disease phenotype depends on both the affected gene and the location of the disease-causing PTC.[18] A minimal distance of 50–55 nt between the PTC and the downstream intron is important for efficient nonsense decay.[18,27–29] If the mutation was located at fewer than 50–55 nt before the last intron, NMD would not occur, and the truncated protein would be translated. NMD may exert a beneficial, neutral or harmful effect, depending on the location of the PTCs in the transcript and the properties of the truncated protein. If the truncated mutant protein has dominant-negative activity, NMD can confer a protective effect that benefits heterozygous carriers of PTCs. By contrast, NMD can also contribute to a disease phenotype when it inhibits the expression of partially functional proteins.[18] In the case of *BCOR* mutations, all of the affected patients have similar phenotypes, irrespective of the location of the mutation, although the phenotypes differ in severity. This observation suggests that the pathogenesis might be haploinsufficiency rather than a dominant negative effect of mutant proteins. It was reported that the truncated OFCD protein in affected patients showed repressor effects equivalent to those of wild-type *BCOR*.[3] Therefore, we hypothesized that the mutant *BCOR* proteins would have partially functional effects and that the abnormal phenotypes observed in the affected tissues were the result of NMD of mutant RNAs, which would result in haploinsufficiency.

Different tissues have different NMD efficiencies. This situation could result in a selective effect in which only NMD-sensitive tissues become abnormal, which is consistent with the typical characteristics of OFCD syndrome. We focused our study on the tooth root, which becomes hyperactive and much longer than normal in OFCD-affected patients. During tooth root development, all functional hard tissues are formed by three types of cells: Hertwig's epithelial root sheath, dental papilla mesenchymal and dental follicle cells, which form developing apical complexes.[30–32] Developing apical complexes are located in the apical region of the developing tooth and can develop into an entire tooth root *in vitro*, without a crown.[33] Mice studies showed that Hertwig's epithelial root sheath cells are detectable on the surface of the root throughout root formation and do not disappear.[33] Most of the Hertwig's epithelial root sheath cells are attached to the surface of the cementum, and others separate to become the epithelial rest of Malassez. Thus, we used the PDL cells surrounding the apical 1/3 and apical pulp cells, which are assumed to comprise all developing apical complexes, for studying hyperactive root formation in OFCD patients. We found that *BCOR* mutations did not affect the expression of the mesenchymal and epithelial cell

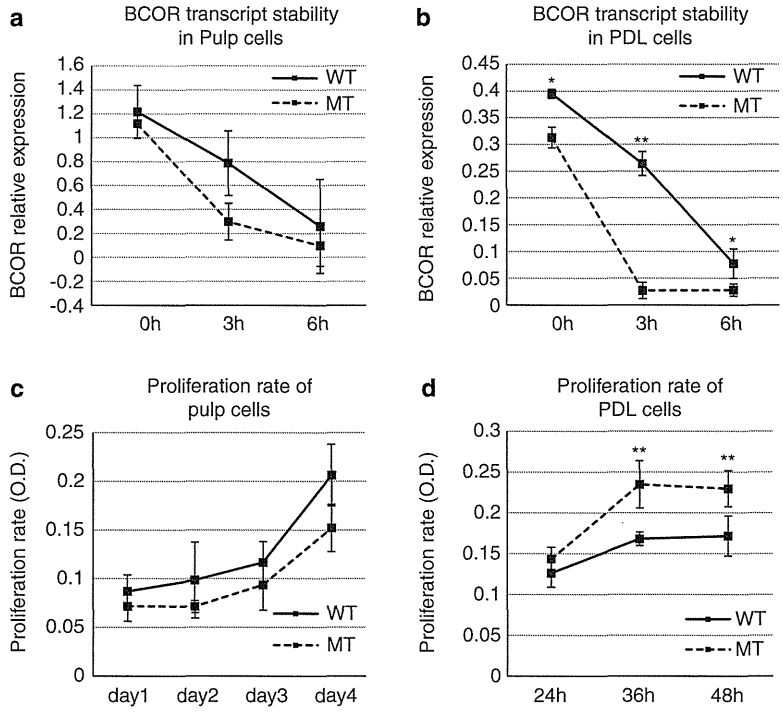

Figure 4 *BCOR* transcript stability and cell proliferation rate. (**a**) *BCOR* transcript stability in pulp cells. (**b**) *BCOR* transcript stability in PDL cells. (**c**) Proliferation rate of pulp cells. (**d**) Proliferation rate of PDL cells. WT, wild-type; MT, mutant. $*P<0.05$, $**P<0.01$.

markers *VIM* and *KRT14*, respectively, in our cultured cells. Mesenchymal and epithelial markers were more highly expressed in cultured PDL cells than in pulp culture. Moreover, cultured PDL cells also showed higher *BCOR* expression than pulp cells, whether wild-type or mutant. It was previously reported that *BCOR* expressed in the mesenchyme has an important role in proper tooth formation.[15] Therefore, our results suggested that *BCOR* is highly expressed in the mesenchyme and that our cultured PDL expressed *BCOR* at higher levels than pulp cells because of the predominance of mesenchymal cells in the PDL cultures. Compared with wild-type, *BCOR* expression was normal in pulp but reduced in PDL cells, which was consistent with our finding of higher rates of NMD in PDL. Moreover, in PDL but not pulp cell cultures, the mutant PDL had unstable mutant transcripts and proliferated faster than wild-type cells. This evidence suggests that the mutant PDL cells have insufficient *BCOR* function to repress target genes, resulting in the promotion of cell proliferation that contributes to hyperactive root formation.

In a previous report, mutant *BCOR* transcript levels did not significantly differ from normal, and mutant MSCs proliferated faster than control cells.[2] That study used MSCs from the root apical papilla of an OFCD patient, and these cells may have different phenotypes than the differentiated pulp or PDL cells used in the present study, although our PDL cells were also harvested from the apical 1/3 and may have included apical papilla cells. Further studies are needed. However, the current study revealed that PDL cells might be more involved than pulp cells in the pathogenesis of radiculomegaly resulting from *BCOR* mutations. The mechanism and function will be studied further.

CONCLUSION

The nonsense mutation in patient 1 and the frameshift mutation in patient 2 were found to contribute to OFCD syndrome. A variation in phenotype severity was observed, and thus, further studies of factors such as X-chromosome inactivation or epigenetic modifications are needed to clarify the genotype–phenotype relationship. In patient 2, the mutation leading to the PTC-induced NMD mechanism in PDL cells caused unstable mutant transcripts and increased cell proliferation, which may be involved in hyperactive root formation.

ACKNOWLEDGEMENTS

This work was supported by a Grant-in-Aid for young scientists (B); 22792038 from JSPS and the GCOE program at Tokyo Medical and Dental University. We would like to thank Dr Kerstin Kutsche, Universitatsklinikum Hamburg-Eppendorf, Hamburg, Germany, and Dr Hitoyata Shimokawa, Tokyo Medical and Dental University, Tokyo, Japan, for their kind advice. We also thank all patients and appreciate their cooperation.

1 Hedera, P. & Gorski, J. L. Oculo-facio-cardio-dental syndrome: skewed X chromosome inactivation in mother and daugther suggest X-linked dominant inheritance. *Am. J. Med. Genet. A.* **123A,** 261–266 (2003).
2 Fan, Z., Yamaza, T., Lee, J. S., Yu, J., Wang, S., Fan, G. *et al.* BCOR regulates mesenchymal stem cell function by epigenetic mechanisms. *Nat. Cell. Biol.* **11,** 1002–1009 (2009).
3 Ng, D., Thakker, N., Corcoran, C. M., Donnai, D., Perveen, R., Schneider, A. *et al.* Oculofaciocardiodental and Lenz microphthalmia syndromes result from distinct classes of mutations in BCOR. *Nat. Genet.* **36,** 411–416 (2004).
4 Davoody, A., Chen, I.-P., Nanda, R., Uribe, F. & Reichenberger, E. J. Oculofaciocardio-dental (OFCD) syndrome: a rare case and review of the literature. *Cleft Palate Craniofac. J.* **49,** e55–e60 (2012).
5 Hilton, E., Johnston, J., Whalen, S., Okamoto, N., Hatsukawa, Y., Nishio, J. *et al.* BCOR analysis in patients with OFCD and Lenz microphthalmia syndromes, mental retardation with ocular anomalies, and cardiac laterality defects. *Eur. J. Hum. Genet.* **17,** 1325–1335 (2009).
6 Oberoi, S., Winder, A. E., Johnston, J., Vargervik, K. & Slavotinek, A. M. Case reports of oculofaciocardiodental syndrome with unusual dental findings. *Am. J. Med. Genet. A.* **136,** 275–277 (2005).

7 Horn, D., Chyrek, M., Kleier, S., Luttgen, S., Bolz, H., Hinkel, G. K. *et al.* Novel mutations in BCOR in three patients with oculo-facio-cardio-dental syndrome, but none in Lenz microphthalmia syndrome. *Eur. J. Hum. Genet.* **13,** 563–569 (2005).
8 Schulze, B. R., Horn, D., Kobelt, A., Tariverdian, G. & Stellzig, A. Rare dental abnormalities seen in oculo-facio-cardio-dental (OFCD) syndrome: three new cases and review of nine patients. *Am. J. Med. Genet.* **82,** 429–435 (1999).
9 Huynh, K. D., Fischle, W., Verdin, E. & Bardwell, V. J. BCoR, a novel co-repressor involved in BCL-6 repression. *Genes Dev.* **14,** 1810–1823 (2000).
10 Forrester, S., Kovach, M. J., Reynolds, N. M., Urban, R. & Kimonis, V. Manifestations in four males with and an obligate carrier of the Lenz microphthalmia syndrome. *Am. J. Med. Genet.* **98,** 92–100 (2001).
11 Ng, D., Hadley, D. W., Tifft, C. J. & Biesecker, L. G. Genetic heterogeneity of syndromic X-linked recessive microphthalmia-anophthalmia: is Lenz microphthalmia a single disorder? *Am. J. Med. Genet.* **110,** 308–314 (2002).
12 Wamstad, J. A. & Bardwell, V. J. Characterization of Bcor expression in mouse development. *Gene Expr. Patterns* **7,** 550–557 (2007).
13 Hilton, E. N., Manson, F. D., Urquhart, J. E., Johnston, J. J., Stavotinek, A. M., Hedera, P. *et al.* Left-sided embryonic expression of the BCL-6 corepressor, BCOR, is required for vertebrate laterality determination. *Hum. Mol. Genet.* **16,** 1773–1782 (2007).
14 Wamstad, J. A., Corcoran, C. M., Keating, A. M. & Bardwell, V. J. Role of the transcriptional corepressor Bcor in embryonic stem cell differentiation and early embryonic development. *PLoS ONE* **3,** e2814 (2008).
15 Cai, J., Kwak, S., Lee, J.-M., Kim, E.-J., Lee, M.-J., Park, G.-H. *et al.* Function analysis of mesenchymal Bcor in tooth develoment by using RNA interference. *Cell. Tissue. Res.* **341,** 251–258 (2010).
16 Linde, L., Boelz, S., Neu-Yilik, G., Kulozik, A. E. & Kerem, B. The efficiency of nonsense-mediated mRNA decay is an inherent character and varies among different cells. *Eur. J. Hum. Genet.* **15,** 1156–1162 (2007).
17 Dedman, A. M., Majeed, Y., Tumova, S., Zeng, F., Kumar, B., Munsch, C. *et al.* TRPC1 transcript variants, inefficient nonsense-mediated decay and low up-frameshift-1 in vascular smooth muscle cells. *BMC. Mol. Biol.* **12,** 30 (2011).
18 Holbrook, J. A., Neu-Yilik, G., Hentze, M. W. & Kulozik, A. E. Nonsense-mediated decay approaches the clinic. *Nat. Genet.* **36,** 801–808 (2004).
19 Tsukawaki, H., Tsuji, M., Kawamoto, T. & Ohyama, K. Three cases of oculo-facio-cardio-dental (OFCD) syndrome. *Cleft Palate Craniofac. J.* **42,** 467–476 (2005).
20 Schwarz, J. M., Rödelsperger, C., Schuelke, M. & Seelow, D. MutationTaster evaluates disease-causing potential of sequence alterations. *Nat. Methods* **7,** 575–576 (2010).
21 Song, J. S., Hwang, D. H., Kim, S.-O., Jeon, M., Choi, B.-J., Jung, H.-S. *et al.* Comparative gene expression analysis of the human periodontal ligament in deciduous and permanent teeth. *PLoS ONE* **8,** e61231 (2013).
22 Huang, A H-C, Chen, Y.-K., Lin, L.-M., Shieh, T.-Y. & Chan, A W-S Isolation and characterization of dental pulp stem cells from a supernumerary tooth. *J. Oral. Pathol. Med.* **37,** 571–574 (2008).
23 Chen, Y. K., Huang, A. H., Chan, A. W. & Lin, L. M. Human dental pulp stem cells derived from cryopreserved dental pulp tissues of vital extracted teeth with disease demonstrate hepatic-like differentiation. *J. Tissue. Eng. Regen. Med.* (2013).
24 Carter, M. S., Doskow, J., Morris, P., Li, S., Nhim, R. P., Sandstedt, S. *et al.* A regulatory mechanism that detects premature nonsense codons in T-cell receptor transcripts in vivo is reversed by protein synthesis inhibitors in vitro. *J. Biol. Chem.* **270,** 28995–29003 (1995).
25 Nelson, S. J. & Ash, M. M. *Wheeler's Dental Anatomy, Physiology and Occlusion.* 9 edn. (Saunders Elsevier, Missouri, USA, 2010).
26 Lozic, B., Ljubkovic, J., Panduric, D. G., Saltvig, I., Kutsche, K., Krzelj, V. *et al.* Oculo-facio-cardio-dental syndrome in three succeeding generations: genotypic data and phenotypic features. *Braz. J. Med. Biol. Res.* **45,** 1315–1319 (2012).
27 Frischmeyer, P. A. & Dietz, H. C. Nonsense-mediated mRNA decay in health and disease. *Hum. Mol. Genet.* **8,** 1893–1900 (1999).
28 Zhang, J., Sun, X., Qian, Y. & Maquat, L. E. Intron function in the nonsense-mediated decay of beta-globin mRNA: indications that pre-RNA splicing in the nucleus can influence mRNA translation in the cytoplasm. *RNA* **4,** 801–815 (1998).
29 Zhang, J., Sun, X., Qian, Y., LaDuca, J. P. & Maquat, L. E. At least one intron is required for the nonsense-mediated decay of triosephosphate isomerase mRNA: possible link between nuclear splicing and cytoplasmic translation. *Mol. Cell. Biol.* **18,** 5272–5283 (1998).
30 Huang, X., Bringas, P. Jr, Slavkin, H. C. & Chai, Y. Fate of HERS during tooth root development. *Dev. Biol.* **334,** 22–30 (2009).
31 Xu, L., Tang, L., Jin, F., Liu, X. H., Yu, J. H., Wu, J. J. *et al.* The apical region of developing tooth root constitutes a complex and maintains the ability to generate root and periodontium-like tissues. *J. Periodontal Res.* **44,** 275–282 (2009).
32 Fang, J., Tang, L., Liu, X. H., Wen, L. Y. & Jin, Y. Changes of the unique odontogenic properties of rat apical bud cells under the developing apical complex microenvironment. *Int. J. Oral Sci.* **1,** 26–33 (2009).
33 Huang, X. F. & Chai, Y. Molecular regulatory mechanism of tooth root development. *Int. J. Oral Sci.* **4,** 177–181 (2012).

CLINICAL REPORT

AMERICAN JOURNAL OF medical genetics PART A

A Novel Heterozygous *MAP2K1* Mutation in a Patient with Noonan Syndrome with Multiple Lentigines

Eriko Nishi,[1,2] Seiji Mizuno,[3] Yuka Nanjo,[4] Tetsuya Niihori,[4] Yoshimitsu Fukushima,[2] Yoichi Matsubara,[4,5] Yoko Aoki,[4] and Tomoki Kosho[1,2]*

[1]Division of Medical Genetics, Nagano Children's Hospital, Azumino, Japan

[2]Department of Medical Genetics, Shinshu University School of Medicine, Matsumoto, Japan

[3]Department of Pediatrics, Central Hospital, Aichi Human Service Center, Kasugai, Japan

[4]Department of Medical Genetics, Tohoku University School of Medicine, Sendai, Japan

[5]National Research Institute for Child Health and Development, Tokyo

Manuscript Received: 31 March 2014; Manuscript Accepted: 1 October 2014

Noonan syndrome with multiple lentigines (NSML), formerly referred to as LEOPARD syndrome, is a rare autosomal-dominant condition, characterized by multiple lentigines, electrocardiographic conduction abnormalities, ocular hypertelorism, pulmonary stenosis, abnormal genitalia, growth retardation, and sensorineural deafness. To date, *PTPN11*, *RAF1*, and *BRAF* have been reported to be causal for NSML. We report on a 13-year-old Japanese boy, who was diagnosed with NSML. He was found to have a novel heterozygous missense variant (c.305A > G; p.E102G) in *MAP2K1*, a gene mostly causal for cardio-facio-cutaneous syndrome (CFCS). He manifested fetal macrosomia, and showed hypotonia and poor sucking in the neonatal period. He had mild developmental delay, and multiple lentigines appearing at approximately age 3 years, as well as flexion deformity of knees bilaterally, subtle facial characteristics including ocular hypertelorism, sensorineural hearing loss, and precocious puberty. He lacked congenital heart defects or hypertrophic cardiomyopathy, frequently observed in patients with NSML, mostly caused by *PTPN11* mutations. He also lacked congenital heart defects, characteristic facial features, or intellectual disability, frequently observed in those with CFCS caused by *MAP2K1* or *MAP2K2* mutations. This may be the first patient clinically diagnosed with NSML, caused by a mutation in *MAP2K1*.

Key words: Noonan syndrome with multiple lentigines (NSML); *MAP2K1*; cardio-facio-cutaneous syndrome (CFCS)

How to Cite this Article:
Nishi E, Mizuno S, Nanjo Y, Niihori T, Fukushima Y, Matsubara Y, Aoki Y, Kosho T. 2015. A novel heterozygous *MAP2K1* mutation in a patient with Noonan syndrome with multiple lentigines.
Am J Med Genet Part A 167A:407–411.

INTRODUCTION

Noonan syndrome with multiple lentigines (NSML), formerly referred to as LEOPARD syndrome, is a rare autosomal-dominant multiple congenital anomaly condition, characterized by multiple lentigines, electrocardiographic (ECG) abnormalities, ocular hypertelorism, pulmonary stenosis, genital abnormalities, growth retardation, and sensorineural deafness [Sarkozy et al., 2008; Gelb and Tartaglia, 2010; Martínez-Quintana and Rodríguez-González, 2012]. The diagnosis of NSML is made on clinical grounds by observation of specific features. Standard diagnostic criteria for NSML, proposed by Voron et al. [1976]; included multiple lentigines and two other cardinal features.

Together with Noonan syndrome (NS), Costello syndrome, cardio-facio-cutaneous syndrome (CFCS), and neurofibromatosis type 1, NSML is classified as RASopathy, a disorder affecting the RAS-MAPK signal transduction pathway [Aoki and Matsubara, 2013]. NSML is genetically heterogeneous and three causative genes have been identified, accounting for approximately 95% of affected individuals [Martínez-Quintana and Rodríguez-González, 2012]. Approximately 85% of patients with NSML have heterozygous

Conflict of interest: none.
Grant sponsor: Ministry of Health, Labour and Welfare, Japan; Grant sponsor: Nagano Children's Hospital Research Foundation.
*Correspondence to:
Tomoki Kosho, M.D., Department of Medical Genetics, Shinshu University School of Medicine, 3-1-1 Asahi, Matsumoto 390-8621, Japan.
E-mail: ktomoki@shinshu-u.ac.jp
Article first published online in Wiley Online Library (wileyonlinelibrary.com): 25 November 2014
DOI 10.1002/ajmg.a.36842

missense mutations in the protein-tyrosine phosphatase, non-receptor type 11 (*PTPN11*) gene (OMIM#151100). To date, 11 different *PTPN11* mutations, all localized in the protein-tyrosine phosphatase (PTP) domain, have been reported in NSML, two of which (p.T279C and p.T468M) constitute approximately 65% of the cases [Martínez-Quintana and Rodríguez-González, 2012]. Two unrelated patients with NSML were found to have heterozygous missense mutations in the v-Raf-1 murine leukemia viral oncogene homolog 1 (*RAF1*) gene (p.L613V and p.S257L) (OMIM#611554) [Pandit et al., 2007]. The p.L613V mutation increases kinase activity and enhances downstream ERK activation [Pandit et al., 2007]. Two unrelated patients with NSML had heterozygous missense mutations in the v-Raf murine sarcoma viral oncogene homolog B1 (*BRAF*) gene (p.T241P and p.L245F) (OMIM#613707) [Koudova et al., 2009; Sarkozy et al., 2009].

Mitogen-activated protein kinase 1 (MAP2K1) and MAP2K2 are dual-specificity protein kinases, which function as effectors of the serine/threonine kinase *RAF* family members by phosphorylating

FIG. 1. Clinical photographs of the patient at the age 7 months (A, B), at 2 5/12 years (C, D), and at 11 years (E–K).

and activating ERK proteins. A heterozygous missense mutation in *MAP2K1* is known to be causal for CFCS or NS [Allanson and Roberts, 2011; Rauen, 2012]. To date, all published *MAP2K1* mutations occurred in exons 2, 3, and 6.

In this report, we present a patient clinically diagnosed with NSML, who had a de novo novel and heterozygous *MAP2K1* variant with probable pathogenicity.

CLINICAL REPORT

The patient, a 13-year-old Japanese boy, was the second child of a healthy 30-year-old mother and a healthy 35-year-old nonconsanguineous father. His two brothers were healthy. He was born by normal vaginal delivery at 41 weeks and 4 days of gestation after an uncomplicated pregnancy. His birth weight was 4,350 g (+3.2 SD), length was 51 cm (+1.0 SD), and OFC was 37 cm (+2.6 SD). He showed hypotonia and sucked poorly in the neonatal period. He raised his head at age 3 months, rolled over at 4 months, and sat unsupported at 7 months. He showed no distinctive facial features and only a few lentigines in infancy (Fig. 1A, B).

His growth was impaired with a weight of 8.25 kg (−2.1 SD), height of 76.9 cm (−1.6 SD), and OFC of 45.6 cm (−1.4 SD) at age 1 7/12 years. His weight was 11 kg (−2.5 SD), height was 90.0 cm (−2.4 SD), and OFC was 49 cm (−0.4 SD) at age 2 10/12 years. Lentigines increased on the face and the limbs (Fig. 1C, D). He walked unassisted at age 3 3/12 years, and spoke a two-word sentence at 3 years. His intellectual quotient was 60 at 4 years, and 82 at 7 years. He showed growth acceleration from age 8.5 years, accompanied by a change in voice, and was diagnosed as precocious puberty at 9 years with an advanced bone age of 11.5 years. At age 10 years, his weight was 22.1 kg (−1.5 SD), height was 130 cm (−1.2 SD), and OFC was 51.8 cm (−1.0 SD). He underwent surgical elongation of his hamstrings, which reduced the limitation of bilateral knee extension from −60° degrees to −20° degrees.

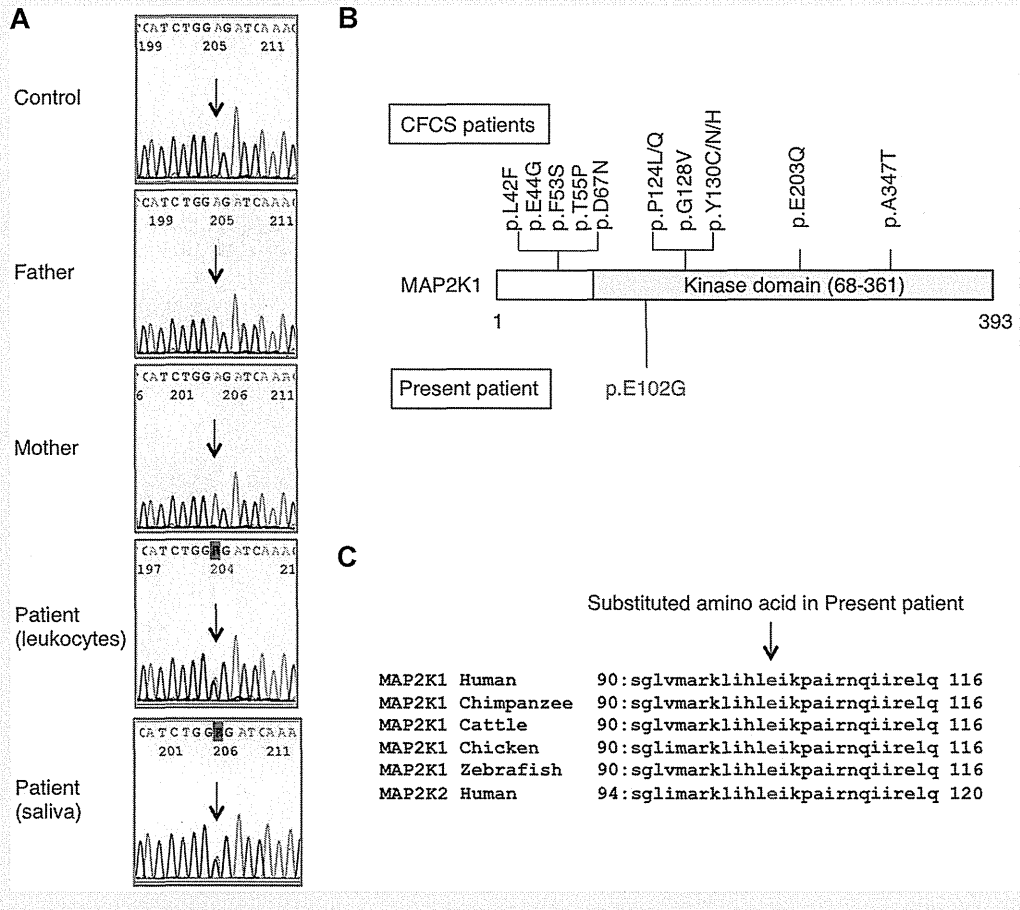

FIG. 2. A: Sanger sequencing of *MAP2K1*, showing an A→G substitution (c.305A > G, p.E102G) in exon 3, which was detected in the patient's DNA from leukocytes and saliva, but not detected in parental samples. B: MAP2K1 domain structure and location of residues altered in the present patient and previously reported patients with cardio-facio-cutaneous syndrome (CFCS). C: MAP2K1 amino acid alignment around the residue where the present amino acid change occurred. This residue is evolutionally conserved.

At age 11 years, his facial features included ocular hypertelorism, a long philtrum, thick upper and lower lip vermilions, and thickened ear helices (Fig. 1E, F). He had hyperextensible and dark skin with multiple lentigines all over the body, several café-au-lait spots, and fine wrinkles on the palms (Fig. 1G–J). He had a slender habitus with pectus carinatum, mild scoliosis, slender extremities, and limited extension of both elbows and knees (Fig. 1K). His weight was 23.0 kg (−1.8 SD) and height was 141 cm (−0.4 SD).

He had no abnormalities in the external genitalia. Resting or 24-hour ECG detected no conduction abnormalities. Echocardiography showed no congenital heart defects, pulmonary valve stenosis, or hypertrophic cardiomyopathy (HCM). Brain magnetic resonance imaging showed no structural abnormalities. He had bilateral mild sensorineural hearing loss with the threshold of 40 dB at approximately 2 kHz. G-banded chromosomes were normal.

MOLECULAR INVESTIGATION

Genomic DNA was isolated from the patient's leukocytes and saliva and his parents' leukocytes after appropriate informed consent. All coding exons and flanking introns in *PTPN11*, *KRAS*, *HRAS*, and *SOS1*, exons 6 and 11–16 in *BRAF*, exons 7, 14, and 17 in *RAF1*, exons 2 and 3 in *MAP2K1/2*, and exon 1 in *SHOC2* were amplified by polymerase chain reaction (PCR) with primers based on GenBank sequences. The primer sequences are available on request. PCR amplification was performed under standard condition using Taq DNA polymerase. After amplification, the PCR products were gel-purified and sequenced on the ABI 3500xL automated DNA sequencer (Applied Biosystems, Carlsbad, CA). A heterozygous missense variant (c.305A > G, p.E102G) was identified in exon 3 of *MAP2K1* in the patient's DNA extracted from his leukocytes and saliva. The variant was not detected in the parental samples (Fig. 2A). No mutation, other than c.305A > G in *MAP2K1*, was identified by the analysis using custom HaloPlex panel (Agilent Technologies, Santa Clara, CA) designed to identify mutations in exons and exon-intron boundaries of the following RASopathy-related genes: *PTPN11*, *HRAS*, *KRAS*, *NRAS*, *BRAF*, *RAF1*, *MAP2K1/2*, *SOS1*, *SHOC2*, *CBL*, *RIT1*, *NF1*, *SPRED1*, and *RRAS*.

DISCUSSION

The present patient had multiple lentigines, café-au-lait spots, ocular hypertelorism, growth impairment, sensorineural hearing loss, hypotonia, low average intelligence, and skeletal abnormalities.

TABLE I. Clinical Features of the Present Patient, Patients With Noonan Syndrome With Multiple Lentigines (NSML), and Patients With Cardio-Facio-Cutaneous Syndrome (CFCS) Caused by *MAP2K1* or *MAP2K2* Mutations

	Present patient	Patients with NSML [Gelb and Tartaglia, 2010]	Patients with CFCS caused by *MAP2K1* or *MAP2K2* mutations [Dentici et al., 2009]	
Causative gene	*MAP2K1*	*PTPN11* (90%) *RAF1* (n = 2) *BRAF* (n = 2)	*MAP2K1* (n = 41)	*MAP2K2* (n = 20)
Sex	Male	Male > Female	Male:Female = 9:14	
Nevi/lentigines	+	<100%	11/34 (32%)	
Café-au-lait spots	+	70–80%	5/30 (17%)	
Congenital heart defects	−	85%	25/39 (64%)	
HCM	−	70%	14/42 (33%)	
ECG abnormalities	−	23%	2/28 (7%)	
Pulmonary valve stenosis	−	25%	17/42 (40%)	
Polyhydramnios	−		20/32 (63%)	
Fetal macrosomia	+		13/25 (52%)	
Short stature	+	<50%	30/38 (79%)	
Macrocephaly	+		26/34 (76%)	
Hypertelorism	+		23/30 (77%)	
Thickened helix	+		27/30 (90%)	
Sparse hair	−		33/49 (67%)	
Sparse eyebrow	−		35/38 (92%)	
Palpebral ptosis	−		18/27 (67%)	
Flat nasal bridge	−		10/12 (83%)	
Joint limitation	+			
Failure to thrive	+		29/35 (83%)	
Intellectual disability	−	30%	43/46 (93%)	
Development delay	+		43/45 (96%)	
Hypotonia	+		40/45 (89%)	
Sensorineural hearing loss	+	<20%		
Seizures	−		16/44 (36%)	

CFCS, cardio-facio-cutaneous syndrome; ECG, electrocardiograph; HCM, hypertrophic cardiomyopathy , NSML, Noonan syndrome with multiple lentigines.

He lacked ECG conduction abnormalities, pulmonary stenosis, or abnormal genitalia. These findings were compatible with the standard diagnosis of NSML by Voron et al. [1976]. The variant c.305A > G, p.E102G was found de novo and not detected in db SNP Release 137 (http://www.ncbi.nlm.nih.gov/projects/SNP/), the Exome Sequencing Project (NHLBI-ESP) database (ESP6500SI-V2) (http://evs.gs.washington.edu/EVS/), the 1000 Genomes Project (1KGP) (http://www.1000genomes.org/), or the Human Gene Mutation Database (http://www.hgmd.cf.ac.uk/ac/index.php). In the COSMIC database, c.302_307delTGGAGA, resulting in an in-frame deletion (p.E102_I103delEI), has been identified in two samples with malignant melanoma and lung cancer (http://cancer.sanger.ac.uk/cancergenome/projects/cosmic/). The glutamine residue at codon 102 is located in the kinase domain (residues 68–361) of *MAP2A1* (Fig. 2B) and is conserved in higher organisms (Fig. 2C). Polymorphism Phenotyping v2 (PolyPhen-2) (http://genetics.bwh.harvard.edu/pph2/) predicts the variant to be possibly damaging, with a score of 0.711. In view of this evidence, the variant p.E102G may be causal for various clinical features consistent with NSML in the patient. However, no functional characterization of the variant was available and Sorting Intolerant From Tolerant (SIFT) (http://sift.jcvi.org) predicts the variant to be tolerated, with a score of 0.09.

We reviewed clinical features of the present patient, previously reported patients with NSML caused by *PTPN11* mutations in most (including two caused by *RAF1* mutations and two caused by *BRAF* mutations), and patients with CFCS caused by *MAP2K1* or *MAP2K2* mutations (Table I) [Pandit et al., 2007; Dentici et al., 2009; Koudova et al., 2009; Sarkozy et al., 2009]. Patients with NSML frequently had congenital heart defects and/or HCM, and sometimes had pulmonary valve stenosis and/or ECG abnormalities [Wakabayashi et al., 2011; Martínez-Quintana and Rodríguez-González, 2012], none of which were found in the present patient. Both patients with NSML caused by *RAF1* mutations had HCM, additionally, one had pulmonary valve stenosis, and the other had a mitral valve anomaly [Pandit et al., 2007]. One of the two patients with NSML caused by *BRAF* mutations had tetralogy of Fallot and the other had mitral and aortic valve dysplasia [Koudova et al., 2009; Sarkozy et al., 2009]. Patients with CFCS caused by *MAP2K1* or *MAP2K2* mutations frequently had congenital heart defects, polyhydramnios, characteristic facial "coarseness" (sparse hair/eyebrows, palpebral ptosis, and flat nasal bridge), and intellectual disability [Dentici et al., 2009], which were not found in the present patient. They rarely or sometimes had nevi, café-au-lait spots, or sensorineural hearing loss [Dentici et al., 2009], which were found in the present patient. Fetal macrosomia, postnatal failure to thrive/growth impairment, macrocephaly, hypotonia, developmental delay, and facial features including hypertelorism and thickened helices were shared by the present patient and over half of the patients with CFCS caused by *MAP2K1* or *MAP2K2* mutations.

In conclusion, the present patient may be the first to fit the standard clinical diagnostic criteria for NSML by Voron et al. [1976]; associated with a *MAP2K1* mutation. He lacked congenital heart defects or HCM, frequently observed in those with NSML, mostly caused by *PTPN11* mutations. He had fetal macrosomia, postnatal failure to thrive/growth impairment, macrocephaly, hypotonia, developmental delay, and hypertelorism but lacked congenital heart defect, characteristic facial features, or intellectual disability; which are frequently observed features in CFCS caused by *MAP2K1* or *MAP2K2* mutations. These observations could offer new insight into the phenotypic spectrum of RASopathies.

ACKNOWLEDGMENTS

We thank the patient and his parents for participating in this study. This work was supported by Research on Intractable Diseases from Ministry of Health, Labour and Welfare, Japan (Y.M., K.T.) and Nagano Children's Hospital Research Foundation (E.N.).

REFERENCES

Allanson JE, Roberts AE. 2011. Noonan syndrome. In: Pagon RA, Adam MP, Bird TD, et al., editors. GeneReviews® [Internet]. Seattle (WA): University of Washington; 1993–2014. Available from: http://www.ncbi.nlm.nih.gov/books/NBK1116/. Accessed March 16, 2014. .

Aoki Y, Matsubara Y. 2013. Ras/MAPK syndromes and childhood hematooncological diseases. Int J Hematology 97:30–36.

Dentici ML, Sarkozy A, Pantaleoni F, Carta C, Lepri F, Ferese R, Cordeddu V, Martinelli S, Briuglia S, Digilio MC, Zampino G, Tartaglia M, Dallapiccola B. 2009. Spectrum of MEK1 and MEK2 gene mutations in cardio-facio-cutaneous syndrome and genetype-phenotype correlations. Eur J Hum Genet 17:733–740.

Gelb BD, Tartaglia M. 2010. LEOPARD syndrome. In: Pagon RA, Adam MP, Bird TD, et al., editors. GeneReviews® [Internet]. Seattle (WA): University of Washington; 1993–2014. Available from: http://www.ncbi.nlm.nih.gov/books/NBK1116/. Accessed March 16, 2014. .

Koudova M, Seemanova E, Zenker M. 2009. Novel BRAF mutation in a patient with LEOPARD syndrome and normal intelligence. Eur J Med Genet. 52:337–340.

Martínez-Quintana E, Rodríguez-González F. 2012. LEOPARD syndrome: Clinical features and gene mutations. Mol Syndromol 3:145–157.

Pandit B, Sarkozy A, Pennacchio LA, Carta C, Oishi K, Martinelli S, Pogna EA, Schackwitz W, Ustaszewska A, Landstrom A, Bos JM, Ommen SR, Esposito G, Lepri F, Faul C, Mundel P, López Siguero JP, Tenconi R, Selicorni A, Rossi C, Mazzanti L, Torrente I, Marino B, Digilio MC, Zampino G, Ackerman MJ, Dallapiccola B, Tartaglia M, Gelb BD. 2007. Gain-of-function RAF1 mutations cause Noonan and LEOPARD syndromes with hypertrophic cardiomyopathy. Nat Genet 39:1007–1012.

Rauen KA. 2012. Cardiofaciocutaneous syndrome. In: Pagon RA, Adam MP, Bird TD, et al., editors. GeneReviews® [Internet]. Seattle (WA): University of Washington; 1993–2014. Available from: http://www.ncbi.nlm.nih.gov/books/NBK1116/. Accessed March 16, 2014. .

Sarkozy A, Digilio MC, Dallapiccola B. 2008. Leopard syndrome. Orphanet J Rare Dis 3:13.

Sarkozy A, Carta C, Moretti S, Zampino G, Digilio MC, Pantaleoni F, Scioletti AP, Esposito G, Cordeddu V, Lepri F, Petrangeli V, Dentici ML, Mancini GM, Selicorni A, Rossi C, Mazzanti L, Marino B, Ferrero GB, Silengo MC, Memo L, Stanzial F, Faravelli F, Stuppia L, Puxeddu E, Gelb BD, Dallapiccola B, Tartaglia M. 2009. Germline BRAF mutations in Noonan, LEOPARD, and cardiofaciocutaneous syndromes: Molecular diversity and associated phenotypic spectrum. Hum Mutat 30:695–702.

Voron DA, Hatfield HH, Kalkhoff RK. 1976. Multiple lentigines syndrome. Case report and review of the literature. Am J Med 60:447–456.

Wakabayashi Y, Yamazaki K, Narumi Y, Fuseya S, Horigome M, Wakui K, Fukushima Y, Matsubara Y, Aoki Y, Kosho T. 2011. Implantable cardioverter defibrillator for progressive hypertrophic cardiomyopathy in a patient with LEOPARD syndrome and a novel PTPN11 mutation Gln510His. Am J Med Genet A 155A:2529–2533.

EJHG Open

European Journal of Human Genetics (2015), 1–11

www.nature.com/ejhg

ARTICLE

Comprehensive clinical studies in 34 patients with molecularly defined UPD(14)pat and related conditions (Kagami–Ogata syndrome)

Masayo Kagami[1], Kenji Kurosawa[2], Osamu Miyazaki[3], Fumitoshi Ishino[4], Kentaro Matsuoka[5] and Tsutomu Ogata*[,1,6]

Paternal uniparental disomy 14 (UPD(14)pat) and epimutations and microdeletions affecting the maternally derived 14q32.2 imprinted region lead to a unique constellation of clinical features such as facial abnormalities, small bell-shaped thorax with a coat-hanger appearance of the ribs, abdominal wall defects, placentomegaly, and polyhydramnios. In this study, we performed comprehensive clinical studies in patients with UPD(14)pat ($n=23$), epimutations ($n=5$), and microdeletions ($n=6$), and revealed several notable findings. First, a unique facial appearance with full cheeks and a protruding philtrum and distinctive chest roentgenograms with increased coat-hanger angles to the ribs constituted the pathognomonic features from infancy through childhood. Second, birth size was well preserved, with a median birth length of ±0 SD (range, −1.7 to +3.0 SD) and a median birth weight of +2.3 SD (range, +0.1 to +8.8 SD). Third, developmental delay and/or intellectual disability was invariably present, with a median developmental/intellectual quotient of 55 (range, 29–70). Fourth, hepatoblastoma was identified in three infantile patients (8.8%), and histological examination in two patients showed a poorly differentiated embryonal hepatoblastoma with focal macrotrabecular lesions and well-differentiated hepatoblastoma, respectively. These findings suggest the necessity of an adequate support for developmental delay and periodical screening for hepatoblastoma in the affected patients, and some phenotypic overlap between UPD(14)pat and related conditions and Beckwith–Wiedemann syndrome. On the basis of our previous and present studies that have made a significant contribution to the clarification of underlying (epi)genetic factors and the definition of clinical findings, we propose the name 'Kagami–Ogata syndrome' for UPD(14)pat and related conditions.
European Journal of Human Genetics (2015) **00**, 1–11. doi:10.1038/ejhg.2015.13

INTRODUCTION

Human chromosome 14q32.2 carries a cluster of imprinted genes including paternally expressed genes (*PEGs*) such as *DLK1* and *RTL1*, and maternally expressed genes (*MEGs*) such as *MEG3* (alias, *GTL2*), *RTL1as* (*RTL1* antisense), *MEG8*, *snoRNAs*, and *microRNAs* (Supplementary Figure S1).[1,2] The parental origin-dependent expression patterns are regulated by the germline-derived primary *DLK1-MEG3* intergenic differentially methylated region (IG-DMR) and the postfertilization-derived secondary *MEG3*-DMR.[2,3] Both DMRs are hypermethylated after paternal transmission and hypomethylated after maternal transmission in the body; in the placenta, the IG-DMR alone remains as a DMR with the same methylation pattern in the body, while the *MEG3*-DMR does not represent a differentially methylated pattern.[2,3] Consistent with such methylation patterns, the hypomethylated IG-DMR and *MEG3*-DMR of maternal origin function as imprinting control centers in the placenta and the body, respectively, and the IG-DMR behaves hierarchically as an upstream regulator for the methylation pattern of the *MEG3*-DMR in the body, but not in the placenta.[3,4]

Paternal uniparental disomy 14 (UPD(14)pat) (OMIM #608149) results in a unique constellation of clinical features such as facial abnormalities, small bell-shaped thorax with coat-hanger appearance of the ribs, abdominal wall defects, placentomegaly, and polyhydramnios.[2,5] These clinical features are also caused by epimutations (hypermethylations) and microdeletions affecting the maternally derived IG-DMR and/or *MEG3*-DMR (Supplementary Figure S1). Such UPD(14)pat and related conditions are rare, with reports of 33 patients with UPD(14)pat, five patients with epimutations, and nine patients with microdeletions (and four new UPD(14)pat patients reported here) (see Supplementary Table S1 for the reference list). For microdeletions, loss of the maternally inherited *MEG3*-DMR alone leads to a typical UPD(14)pat body phenotype and apparently normal placental phenotype,[3,4] whereas loss of the maternally derived IG-DMR alone or both DMRs results in a typical body and placental UPD(14)pat phenotype, consistent with the methylation patterns of the two DMRs.[2,3] Furthermore, correlations between clinical features and deleted segments have indicated the critical role of excessive *RTL1* (but not *DLK1*) expression in phenotypic development.[2,6] Such an excessive *RTL1* expression is primarily due to loss of functional *RTL1as*-encoded *microRNAs* that act as a *trans*-acting repressor for *RTL1* expression.[6] Indeed, the *RTL1* expression level is ~5 times, rather than 2 times, increased in placentas with UPD(14)pat

[1]Department of Molecular Endocrinology, National Research Institute for Child Health and Development, Tokyo, Japan; [2]Division of Medical Genetics, Kanagawa Children's Medical Center, Yokohama, Japan; [3]Department of Radiology, National Center for Child Health and Development, Tokyo, Japan; [4]Department of Epigenetics, Medical Research Institute, Tokyo Medical and Dental University, Tokyo, Japan; [5]Department of Pathology, National Center for Child Health and Development, Tokyo, Japan; [6]Department of Pediatrics, Hamamatsu University School of Medicine, Hamamatsu, Japan
*Correspondence: Dr T Ogata, Department of Pediatrics, Hamamatsu University School of Medicine, Hamamatsu 431-3192, Japan. Tel: +81 53 435 2310; Fax: +81 53 435 2310; E-mail: tomogata@hama-med.ac.jp
Received 30 August 2014; revised 7 January 2015; accepted 14 January 2015

Table 1 Clinical manifestations in 33 Japanese and one Irish patients with UPD(14)pat and related conditions (Kagami–Ogata syndrome)

	UPD(14)pat	*Epimutations*	*Microdeletions*				*Total*
			Subtype 1	*Subtype 2*	*Subtype 3*	*Subtotal*	
	Pts 1–23 (n = 23)	*Pts 24–28 (n = 5)*	*Pts 29–31 (n = 3)*	*Pt 32 (n = 1)*	*Pts 33–34 (n = 2)*	*Pts 29–34 (n = 6)*	*Pts 1–34 (n = 34)*
Age at the last examination or death (y)	2.9 (0.0–15.0)	2.0 (0.8–5.5)	2.8 (0.8–8.9)	(4 days)	4.5 (3.8–5.1)	3.3 (0.0–8.9)	2.8 (0.0–15.0)
Sex (male:female)	9:14	3:2	1:2	0:1	0:2	1:5	13:21
Molecular findings[a]							
IG-DMR of maternal origin	Absent	Methylated	Deleted	Unmethylated	Deleted		
MEG3-DMR of maternal origin	Absent	Methylated[b]	Deleted/methylated[b]	Deleted	Deleted		
DLK1 expression level	2×	2×	1 or 2×	2× (1×)[c]	1 or 2×		
RTL1 expression level	~5×	~5×	~5×	~5× (1× or ~2.5×)[c]	~2.5×		
MEGs expression level	0×	0×	0×	0× (1× or 0×)[c]	0×		
Pregnancy and delivery							
Polyhydramnios	23/23	5/5	3/3	0/1	2/2	5/6	33/34
Gestational age at Dx (w)	25 (14–30)	27.5 (22–30)	Unknown	—	21	21	25.5 (14–30)
Amnioreduction	18/20	4/5	2/3	0/1	1/2	3/6	25/31
Amnioreduction (>30 w)	18/18	4/4	2/2	—	1/1	3/3	25/25[d]
Placentomegaly[e]	14/17	4/4	3/3	0/1	2/2	5/6	23/27
Prenatal Dx of thoracic abnormality	8/20[f]	2/3	0/1	—	0/1	0/2	10/25
Gestational age at Dx (w)	26 (22–33)	27.5 (25–30)	—	—	—	—	26 (22–33)
Prenatal Dx of abdominal abnormality	6/18	3/3	1/1	—	0/1	1/2	10/23
Gestational age at Dx (w)	26 (22–28)	25	Unknown	Unknown	Unknown	Unknown	25.5 (22–28)
Gestational age (w)	34.5 (24–38)	35 (30–37)	30 (27–33)	28	32.5 (30–35)	30 (27–35)	34 (24–38)
Premature delivery (<37 w)	17/23	4/5	3/3	1/1	2/2	6/6	27/34
Delivery (Cesarean:Vaginal)	15:8	4:1	2:1	0:1	2:0	4:2	23:11
Medically assisted reproduction	1/18	0/1	0/1	Unknown	0/1	0/2	1/21
Growth pattern							
Prenatal growth failure[g]	0/23	0/5	0/3	0/1	0/2	0/6	0/34
Prenatal overgrowth[h]	13/23	3/5	3/3	0/1	1/2	4/6	20/34
Birth length (patient number)	21	5	1	1	2	4	30
SD score, median (range)	+0.3 (–1.7 to +3.0)	–0.5 (–0.9 to +1.4)	0.0	–1.1	+0.7 (–0.1 to +1.5)	–0.1 (–1.1 to +1.5)	±0 (–1.7 to +3.0)
Actual length (cm), median (range)	45.0 (30.6 to 51.0)	43.5 (41.0 to 50.0)	43.0	34.0	43.5 (42.0 to 45.0)	42.5 (34.0 to 45.0)	44.7 (30.6 to 51.0)
Birth weight (patient number)	23	5	3	1	2	6	34
SD score, median (range)	+2.2 (+0.1 +8.8)	+2.2 (+0.5 to +3.7)	+2.8 (+2.4 to +3.7)	+1.5	+1.7 (+0.9 to +2.5)	+2.5 (+0.9 to +3.7)	+2.3 (+0.1 to +8.8)
Actual weight (cm), median (range)	2.79 (1.24 to 3.77)	2.9 (1.61 to 3.28)	2.04 (1.30 to 2.84)	1.32	2.24 (1.55 to 2.94)	1.79 (1.30 to 2.94)	2.79 (1.24 to 3.77)
Postnatal growth failure[i]	7/20	2/5	2/3	—	0/2	2/5	11/30
Postnatal overgrowth[j]	1/20	1/5	0/3	—	0/2	0/5	2/30
Present stature (patient number)	20	5	3	—	1	4	29
SD score, median (range)	–1.6 (–8.7 to +1.1)	–1.8 (–7.1 to +0.9)	–2.2 (–3.3 to –1.3)	—	–1.6	–1.9 (–3.3 to –1.3)	–1.6 (–8.7 to +1.1)
Present weight (patient number)	20	5	3	—	2	5	30
SD score, median (range)	–1.0 (–6.0 to +2.4)	–0.6 (–5.5 to +4.0)	–1.3 (–2.2 to ±0)	—	–1.1 (–1.3 to –0.9)	–1.3 (–2.2 to ±0)	–1.0 (–6.0 to +4.0)

Table 1 (Continued)

	UPD(14)pat	*Epimutations*	*Microdeletions*				*Total*
			Subtype 1	*Subtype 2*	*Subtype 3*	*Subtotal*	
	Pts 1–23 (n = 23)	*Pts 24–28 (n = 5)*	*Pts 29–31 (n = 3)*	*Pt 32 (n = 1)*	*Pts 33–34 (n = 2)*	*Pts 29–34 (n = 6)*	*Pts 1–34 (n = 34)*
Craniofaciocervical features							
Frontal bossing	17/22	4/5	1/3	1/1	2/2	4/6	25/33
Hairy forehead	18/22	1/5	3/3	1/1	0/2	4/6	23/33
Blepharophimosis	18/22	3/5	2/3	0/1	1/2	3/6	24/33
Small ears	8/21	2/5	1/3	1/1	0/2	2/6	12/32
Depressed nasal bridge	23/23	5/5	3/3	0/1	1/2	4/6	32/34
Anteverted nares	19/22	4/5	3/3	0/1	2/2	5/6	28/33
Full cheek	20/21	4/4	2/2	0/1	1/1	3/4	27/29
Protruding philtrum	23/23	5/5	3/3	0/1	2/2	5/6	33/34
Puckered lips	11/21	3/5	3/3	0/1	0/2	3/6	17/32
Micrognathia	20/21	5/5	3/3	1/1	1/2	5/6	30/32
Short webbed neck	22/22	5/5	3/3	1/1	2/2	6/6	33/33
Thoracic abnormality							
Small bell-shaped thorax in infancy[k]	23/23	5/5	3/3	1/1	2/2	6/6	34/34
Coat-hanger appearance in infancy[l]	23/23	5/5	3/3	1/1	2/2	6/6	34/34
Laryngomalacia	8/20	2/5	2/3	—	0/1	2/4	12/29
Tracheostomy	7/21	1/4	0/2	—	2/2	2/4	10/29
Mechanical ventilation	21/23	5/5	3/3	1/1	2/2	6/6	32/34
Duration of ventilation (m)[m]	1.2 (0.1–17)	0.7 (0.1–0.9)	5 (0.23–10)	—	1.5 (1–2)	2 (0.2–10)	1.0 (0.1–17)
Abdominal wall defects							
Omphalocele	7/23	2/5	1/3	1/1	0/2	2/6	11/34
Diastasis recti	16/23	3/5	2/3	0/1	2/2	4/6	23/34
Developmental delay							
Developmental delay	21/21	5/5	3/3	—	2/2	5/5	31/31
Developmental/intellectual quotient	55 (29–70)	52 (48–56)	Unknown	Unknown	Unknown	—	55 (29–70)
Delayed head control (>4 m)[n]	14/16	4/4	1/1	—	1/1	2/2	20/22
Age at head control (m)[o]	7 (3–36)	7 (6–11)	6	—	6	6 (6)	7 (3–36)
Delayed sitting without support (>7 m)[n]	16/16	4/4	2/2	—	1/1	3/3	23/23
Age at sitting without support (m)[o]	12 (8–25)	11.5 (10–20)	22.5 (18–27)	—	18	18 (18–27)	12 (8–27)
Delayed walking without support (>14 m)[n]	17/17	3/3	2/2	—	2/2	4/4	24/24
Age at walking without support (m)[o]	25.5 (20–49)	25 (22–39)	60 (30–90)	—	24	30 (24–90)	25.5 (20–90)
Other features							
Feeding difficulty	20/21	5/5	3/3	—	2/2	5/5	30/31
Duration of tube feeding (m)[p]	6 (0.1–72)	8.5 (0.5–17)	59.5 (30–89)	—	51	51 (30–89)	7.5 (0.1–89)
Joint contractures	14/22	3/5	3/3	0/1	0/2	3/6	20/33
Constipation	12/20	3/4	1/2	—	0/2	1/4	16/28
Kyphoscoliosis	9/21	3/5	1/2	0/1	0/1	1/4	13/30

Table 1 (Continued)

	UPD(14)pat	*Epimutations*	*Microdeletions*				*Total*
			Subtype 1	*Subtype 2*	*Subtype 3*	*Subtotal*	
	Pts 1–23 (n = 23)	*Pts 24–28 (n = 5)*	*Pts 29–31 (n = 3)*	*Pt 32 (n = 1)*	*Pts 33–34 (n = 2)*	*Pts 29–34 (n = 6)*	*Pts 1–34 (n = 34)*
Coxa valga	6/21	1/5	3/3	0/1	1/2	4/6	11/32
Cardiac disease	5/22	1/5	0/3	1/1	1/2	2/6	8/33
Inguinal hernia	5/22	1/5	2/3	0/1	0/2	2/6	8/33
Seizure	1/21	0/5	0/3	0/1	0/2	0/6	1/32
Hepatoblastoma	3/23	0/5	0/3	0/1	0/2	0/6	3/34
Mortality within the first 5 years							
Alive:deceased	18:5	5:0	2:1	0:1	1:1	3:3	26:8
Parents							
Paternal age at childbirth (y)	35 (24–47)	30 (26–36)	37 (34–39)	25	31.5 (27–36)	35 (25–39)	34 (24–47)
Maternal age at childbirth (y)	31 (25–43)	28 (25–35)	31 (27–36)	25	30.5 (28–33)	29.5 (25–36)	31 (25–43)
Advanced childbearing age (⩾35 y)	8/23	1/5	1/3	0/1	0/2	1/6	8/34

Abbreviations: CHA, coat-hanger angle; Dx, diagnosis; m, month; M/W, mid to widest thorax diameter; UPD(14), uniparental disomy 14; w, week; y, year.
Patient #32 is Irish, and the remaining patients are Japanese; the Irish patient has also been examined by Beygo *et al.*[4]
Age data are expressed by median and range.
The denominators indicate the number of patients examined for the presence or absence of each feature, and the numerators represent the number of patient assessed to be positive for that feature; thus, differences between the denominators and numeratorsdenote the number of patients evaluated to be negative for the feature.
[a]For details, see Supplementary Figures S1 and S2.
[b]The *MEG3*-DMR is predicted to be grossly hypomethylated in the placenta.
[c]Expression patterns of the imprinted genes are predicted to be different between the body and the placenta in this patient, while they are predicted to be identical between the body and the placenta in other patients (See Supplementary Figure S1).
[d]Amnioreduction was performed about two times in 23 of the 25 pregnancies.
[e]Placental weight >120% of the gestational age-matched mean placental weight.[34]
[f]The diagnosis of UPD(14)pat has been suspected in two patients (patients #7 and #21).
[g]Birth length and/or birth weight < −2 SD of the gestational age- and sex-matched Japanese reference data (http://jspe.umin.jp/medical/keisan.html).
[h]Birth length and/or birth weight >+2 SD of the gestational age- and sex-matched Japanese reference data (http://jspe.umin.jp/medical/keisan.html).
[i]Present length/height and/or present weight < −2 SD of the age- and sex-matched Japanese reference data (http://jspe.umin.jp/medical/taikaku.html).
[j]Present length/height and/or present weight >+2 SD of the age- and sex-matched Japanese reference data (http://jspe.umin.jp/medical/taikaku.html).
[k]The M/W ratio below nromal range (see Figure 2).
[l]The CHA above the normal range (see Figure 2).
[m]The duration in patients in whom mechanical ventilation could be discontinued.
[n]The age when 90% of infants pass each gross motor developmental milestone (based on Revised Japanese Version of Denver Developmental Screening Test) (http://www.dinf.ne.jp/doc/japanese/prdl/jsrd/norma/n175/img/n175_078i01.gif).
[o]The median (range) of ages in patients who passed each gross motor developmental milestone; patients who have not passed each milestone are not included.
[p]The duration in patients in whom tube feeding could be discontinued.

accompanied by two copies of functional *RTL1* and no functional *RTL1as*.[6] This implies that the *RTL1* expression level is ~2.5 times increased in the absence of functional *RTL1as*-encoded *microRNAs*.

Here, we report comprehensive clinical findings in a series of patients with molecularly confirmed UPD(14)pat and related conditions, and suggest pathognomonic and/or characteristic features and their underlying factors. We also propose the name 'Kagami–Ogata syndrome' for UPD(14)pat and related conditions.

MATERIALS AND METHODS

Ethical approval

This study was approved by the Institute Review Board Committee at the National Center for Child Health and Development, and performed after obtaining written informed consent to publish the clinical and molecular information. We also obtained written informed consent with parental signature to publish facial photographs.

Patients

This study consisted of 33 Japanese patients and one Irish patient (patient #32) with UPD(14)pat and related conditions (13 males and 21 females; 31 patients with normal karyotypes and two patients (#17 and #20) with Robertsonian translocations involving chromosome 14 (karyotyping not performed in patient #1); 30 previously described patients[2,3,7–10] and four new patients) in whom underlying (epi)genetic causes were clarified and detailed clinical findings were obtained (Supplementary Table S2).

The 34 patients were classified into three groups according to the underlying (epi)genetic causes that were determined by methylation analysis for the two DMRs, microsatellite analysis for a total of 24 loci widely dispersed on chromosome 14, fluorescence *in situ* hybridization for the two DMRs, and oligonucleotide array-based comparative genomic hybridization for the 14q32.2 imprinted region, as reported previously:[9] (1) 23 patients with UPD(14)pat (UPD-group); (2) five patients with epimutations (Epi-group); and (3) six patients with microdeletions (Del-group) (Supplementary Figure S2).

Furthermore, the 23 patients of UPD-group were divided into three subtypes in terms of UPD generation mechanisms by microsatellite analysis, as reported previously:[9] (1) 13 patients with monosomy rescue (MR) or postfertilization mitotic error (PE)-mediated UPD(14)pat indicated by full isodisomy (subtype 1) (UPD-S1); (2) a single patient with PE-mediated UPD(14)pat demonstrated by segmental isodisomy (subtype 2) (UPD-S2); and (3) nine patients with trisomy rescue (TR) or gamete complementation (GC)-mediated UPD(14)pat revealed by heterodisomy for at least one locus (subtype 3) (UPD-S3) (Supplementary Figure S2) (it is possible that some patients classified as UPD-S1 may have a cryptic heterodisomic region(s) and actually belong to UPD-S3). Similarly, the six patients of Del-group were divided into three subtypes in terms of the measured/predicted *RTL1* expression level in the body and placenta:[2,3] (1) three patients with ~5 times *RTL1* expression level in both the body and placenta (subtype 1) (Del-S1); (2) a single patient with about five times *RTL1* expression level in the body and normal (1 time) or ~2.5 times *RTL1* expression level in the placenta (subtype 2) (Del-S2); and (3) two patients with ~2.5 times *RTL1* expression level in both the body and placenta (subtype 3) (Del-S3) (Supplementary Figure S2). The measured/predicted expression patterns of the imprinted genes in each group/subtype are illustrated in Supplementary Figure S1.

Clinical studies

We used a comprehensive questionnaire to collect detailed clinical data of all patients from attending physicians. To evaluate chest roentgenographic findings, we obtained the coat-hanger angle (CHA) to the ribs and the ratio of the mid to widest thorax diameter (M/W ratio), as reported previously.[11] We also asked the physicians to report any clinical findings not covered by the questionnaire.

Statistical analysis

Statistical significance of the median among three groups and between two groups/subtypes was examined by the Kruskal–Wallis test and the Mann–Whitney's *U*-test, respectively, and that of the frequency among three groups and between two groups was analyzed by the Fisher's exact probability test, using the R environment (http://cran.r-project.org/bin/windows/base/old/2.15.1/). $P<0.05$ was considered significant. Kaplan–Meier survival curves were constructed using the R environment.

RESULTS

Clinical findings of each group/subtype are summarized in Table 1, and those of each patient are shown in Supplementary Table S2. Phenotypic findings were comparable among UPD-S1, UPD-S2, and UPD-S3, and somewhat different among Del-S1, Del-S2, and Del-S3, as predicted from the expression patterns of the imprinted genes (Supplementary Figure S1). Thus, we showed the data of UPD-group (the sum of UPD-S1, UPD-S2, and UPD-S3) and those of each subtype of Del-group (Del-S1, Del-S2, and Del-S3) in Table 1, and described the data of UPD-S1, UPD-S2, and UPD-S3 in Supplementary Table S3.

We registered the clinical information of each patient in the Leiden Open Variation Database (LOVD) (http://www.lovd.nl/3.0/home; http://databases.lovd.nl/shared/individuals), and the details of each microdeletion in the ClinVar Database (http://www.ncbi.nlm.nih.gov/clinvar/). The LOVD Individual IDs and the ClinVar SCV accession numbers are shown in Supplementary Table S2.

Pregnancy and delivery

Polyhydramnios was observed from ~25 weeks of gestation during the pregnancies of all patients, except for patient #32 of Del-S2 who had deletion of the *MEG3*-DMR and three of the seven *MEG3* exons, and usually required repeated amnioreduction, especially after 30 weeks of gestation. Placentomegaly was usually identified in patients affected with polyhydramnios, but not found in three patients of UPD-group. Thoracic and abdominal abnormalities were found by ultrasound studies in ~40% of patients from ~25 weeks of gestation, and UPD(14)pat was suspected in patients #7 and #21, due to delineation of the bell-shaped thorax with coat-hanger appearance of the ribs. Premature delivery was frequently observed, especially in Del-group. Because of fetal distress and polyhydramnios, ⩾two-thirds of the patients in each group were delivered by Cesarean section. Medically assisted reproduction was reported only in one (patient #8) of 21 patients for whom clinical records on conception were available.

Growth pattern

Prenatal growth was characterized by grossly normal birth length and obviously excessive birth weight. Indeed, birth length ranged from 30.6 to 51.0 cm (−1.7 to +3.0 SD for the gestational age- and sex-matched Japanese reference data) with a median of 44.7 cm (±0 SD), and birth weight ranged from 1.24 to 3.77 kg (+0.1 to +8.8 SD) with a median of 2.79 kg (+2.3 SD). Although birth weight was disproportionately greater than birth length, there was no generalized edema as a possible cause of overweight.

In contrast, postnatal growth was rather compromised, and growth failure (present length/height and/or weight < -2 SD) was observed in about one-third of patients of each group. Postnatal weight was better preserved than postnatal length/height.

Craniofaciocervical features

All patients exhibited strikingly similar craniofaciocervical features (Figure 1). Indeed, >90% of patients had depressed nasal bridge, full cheeks, protruding philtrum, micrognathia, and short webbed neck. In particular, the facial features with full cheeks and protruding philtrum

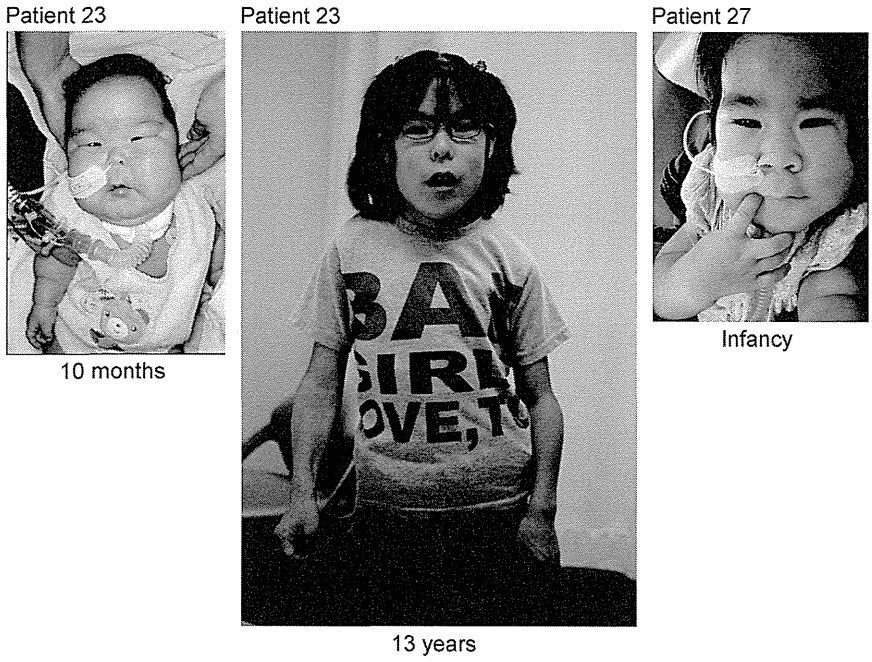

Figure 1 Photographs of patient #23 with UPD(14)pat and patient #27 with epimutation.

appeared to be specific to UPD(14)pat and related conditions, and were recognizable from infancy through childhood.

Thoracic abnormality

The 34 patients invariably showed small bell-shaped small thorax with coat-hanger appearance of the ribs in infancy (Figure 2). Long-term (⩾10 years) follow-up in patient #12 of UPD-group and patient #31 of Del-S1 who had ~5 times of *RTL1* expression, and in patient #34 of Del-S3 who had ~2.5 times of *RTL1* expression, showed that the CHAs remained above the normal range of age-matched control children, while the M/W ratios, though they were below the normal range in infancy, became within the normal range after infancy (Figure 2). Laryngomalacia was also often detected in each group.

Mechanical ventilation was performed in all patients except for patients #14 and #20 of UPD-group, and tracheostomy was also carried out in about one-third of patients. Mechanical ventilation could be discontinued during infancy in 22 patients (Supplementary Figure S3). Ventilation duration was variable with a median period of 1 month among the 22 patients, and was apparently unrelated to the underlying genetic cause or gestational age.

Abdominal wall defects

Omphalocele was identified in about one-third of patients, and diastasis recti was found in the remaining patients.

Developmental status

Developmental delay (DD) and/or intellectual disability (ID) was invariably present in 26 patients examined (age, 10 months to 15 years), with the median developmental/intellectual quotient (DQ/IQ) of 55 (range, 29–70) (Figure 3). Gross motor development was also almost invariably delayed, with grossly similar patterns among different groups. In patients who passed gross motor developmental milestones, head control was achieved at ~7 months, sitting without support at ~12 months, and walking without support at ~2.1 years of age.

Other features

Several prevalent features were also identified. In particular, except for patient #22, feeding difficulty with poor sucking and swallowing was exhibited by all patients who were affected with polyhydramnios, and gastric tube feeding was performed in all patients who survived more than 1 week (Supplementary Figure S4). Tube-feeding duration was variable with a median period of ~7.5 months in 16 patients for whom tube feeding was discontinued, and tended to be longer in Del-group. In addition, there were several features manifested by single patients (Supplementary Table S2).

Notably, hepatoblastoma was identified at 46 days of age in patient #17, at 218 days in patient #18, and at 13 months of age in patient #8 of UPD-group (Figure 4). It was surgically removed in patients #8 and #18, although chemotherapy was not performed because of poor body condition. In patient #17, neither an operation nor chemotherapy could be carried out because of the patient's severely poor body condition. Histological examination of the removed tumors revealed a poorly differentiated embryonal hepatoblastoma with focal macrotrabecular lesions in patient #8 (Figure 4) and a well-differentiated hepatoblastoma in patient #18.[10]

Mortality

Eight patients were deceased before 4 years of age. The survival rate was 78% in UPD-group, 100% in Epi-group, and 50% in Del-group; it was 25% in patients born ⩽29 weeks of gestation, 83% in those born 30–36 weeks of gestation, and 86% in those born ⩾37 weeks of gestation (Figure 5). The cause of death was variable; however, respiratory problems were a major factor, because patient #1 died

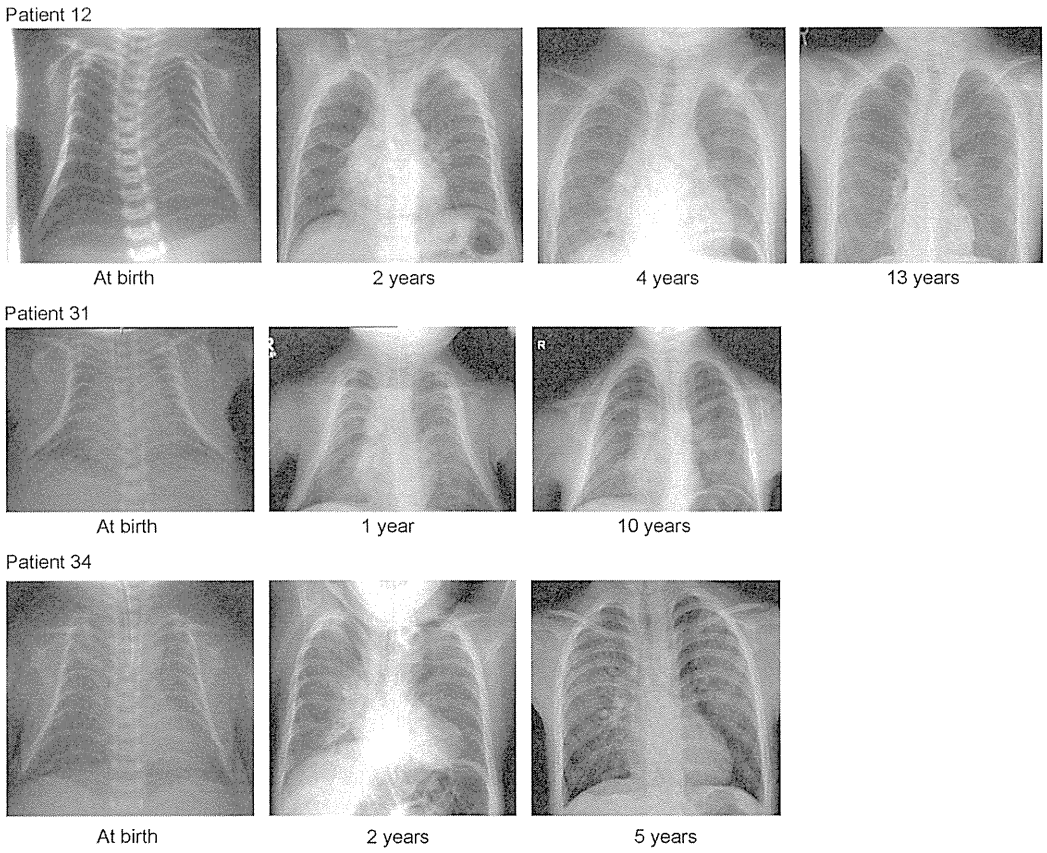

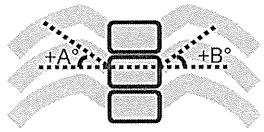

CHA = (A + B) ÷ 2
(6th posterior ribs)

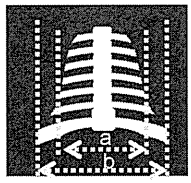

M/W ratio = a / b

		CHA	M/W ratio
Patient 12	At birth	41	70
	2 years	39	88
	4 years	42	94
	13 years	39	92
Patient 31	At birth	35	58
	1 year	28	80
	10 years	29	85
Patient 34	At birth	44	70
	2 year	48	93
	5 years	37	96
UPD(14)pat	At birth	+28 ~ +45	58 ~ 80 (n=8)
	~ 5 years	+25 ~ +45	>78% (n=3)
Controls	At birth	–11 ~ +1.9	82 ~ 89 (n=10)
	~ 5 years	–21 ~ +15	83 ~ 98 (n=10)
	~ 10 years	–9.3 ~ +20	91 ~ 100 (n=10)

Figure 2 Chest roentgenograms of patient #12 of UPD-group, patient #31 of Del-S1, and patient #34 of Del-S3. *RTL1* expression level is predicted to be ~5 times higher in patients #12 and #31, and ~2.5 times higher in patient #34. The CHA to the ribs remains above the normal range throughout the study period, whereas the M/W ratio (the ratio of the mid to widest thorax diameter) normalizes with age.

of neonatal respiratory distress syndrome, and patients #8, #30 and #33 died during a respiratory infection. Of the three patients with hepatoblastoma, patient #17 died of hepatoblastoma, whereas patient #8 died during influenza infection and patient #18 died of hemophagocytic syndrome.

Comparison among/between different groups/subtypes

Clinical findings were grossly similar among/between different groups/subtypes with different expression dosages of *RTL1* and *DLK1*. However, significant differences were found for short gestational age and long duration of tube feeding in Del-group (among three groups

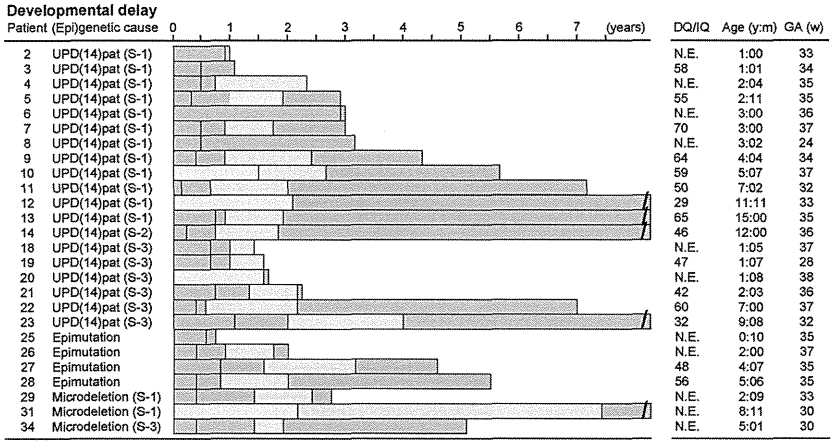

Figure 3 Developmental status. The orange, green, yellow, and blue bars represent the period before head control, the period after head control and before sitting without support, the period after sitting without support and before walking without support, and the period after walking without support, respectively. The gray bars denote the period with no information. DQ, developmental quotient; IQ, intellectual quotient; N.E., not examined; Age, age at the last examination or at death; and GA, gestational age.

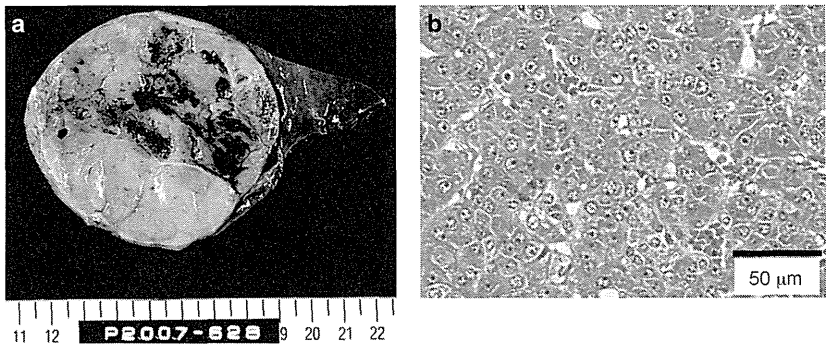

Figure 4 Hepatoblastoma in patient #8 of UPD-group. (**a**) Macroscopic appearance of the hepatoblastoma with a diameter of ~8 cm. (**b**) Microscopic appearance of the hepatoblastoma exhibiting a trabecular pattern. The hepatoblastoma cells are associated with eosinophilic cytoplasm and large nuclei, and resemble fetal hepatocytes.

and against Epi-group and UPD-group) and infrequent hairy forehead in Epi-group (among three groups and against UPD-group) (actual *P*-values are available on request).

DISCUSSION

We examined detailed clinical findings in patients with UPD(14)pat and related conditions. The results indicate that the facial features with full cheeks and protruding philtrum and the thoracic roentgenographic findings with increased CHAs to the ribs represent the pathognomonic features of UPD(14)pat and related conditions from infancy through the childhood. In addition, the decreased M/W ratios also denote the diagnostic hallmark in infancy, but not after infancy. Although other features such as polyhydramnios, placentomegaly, and abdominal wall defects are characteristic of UPD(14)pat and related conditions, they would be regarded as rather nonspecific features that are also observed in other conditions such as Beckwith–Wiedemann syndrome (BWS) (Supplementary Table S4).[12,13]

Such body and placental features were similarly exhibited by patients of each group/subtype, including those of Del-S1, Del-S2, and Del-S3 with different expression dosage of *DLK1* (1× or 2×) and *RTL1* (~2.5× or ~5×), except for patient #32 of Del-S2 who showed typical body features but apparently lacked placental features. Indeed, the difference in the *DLK1* expression dosage had no discernible clinical effects, although mouse *Dlk1* is expressed in several fetal tissues, including the ribs.[14,15] Similarly, in contrast to our previous report which suggested a possible dosage effect of *RTL1* expression level on the phenotypic severity,[2] the difference in the *RTL1* expression dosage turned out to have no recognizable clinical effects after analyzing long-term clinical courses in the affected patients. This suggests that ~2.5× *RTL1* expression is the primary factor for the phenotypic development in the body and placenta. Consistent with the critical role of excessive *RTL1* expression in the phenotypic development, mouse *Rtl1* is clearly expressed in the fetal ribs and skeletal muscles (Supplementary Figure S5) as well as in the placenta,[16,17] and human *RTL1* mRNA and RTL1 protein are strongly expressed in placentas with UPD(14)pat.[6] Thus, lack of placental abnormalities in patient #32 can be explained by assuming a positive *RTL1as* expression and resultant normal (1×) *RTL1* expression in the placenta (Supplementary Figure S1). In addition, since mouse *Gtl2* (*Meg3*) is expressed in multiple fetal tissues including the primordial cartilage,[14] this may argue for the positive role of absent *MEGs* expression in phenotypic development.

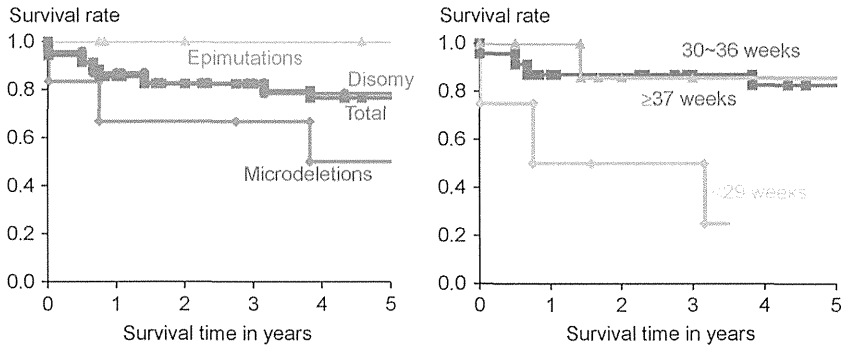

Patient	(Epi)genetic cause	GA	Cause of death	Age of death
1	UPD(14)pat (S-1)	34	Respiratory failure	2 hours
8	UPD(14)pat (S-1)	24	Influenza infection	3 2/12 yrs
15	UPD(14)pat (S-3)	34	Necrotizing enterocolitis	6 mos
17	UPD(14)pat (S-3)	32	Hepatoblastoma	8 mos
18	UPD(14)pat (S-3)	37	Hemophagocytic syndrome	1 5/12 yrs
30	Microdeletion (S-1)	27	Sudden death at URI	9 mos
32	Microdeletion (S-2)	28	Intracranial hemorrhage	4 days
33	Microdeletion (S-3)	35	RS virus infection	3 10/12 yrs

Figure 5 Kaplan–Meier survival curves according to the (epi)genetic cause and the gestational age (week), and summary of the causes of death. GA, gestational age; URI, upper respiratory infection; and RS, respiratory syncytial. Patients #8, #17, and #18 had hepatoblastoma.

The present study revealed several notable findings. First, polyhydramnios was identified during the pregnancies of nearly all patients, except for patient #32 of Del-S2. Amniotic fluid originates primarily from fetal urine and is absorpted primarily by fetal swallowing into the digestive system.[18,19] Since fetal hydration and the resultant urine flow mainly depend on the water flow from maternal circulation across the placenta,[19] placentomegaly would have facilitated the production of amniotic fluid. Furthermore, since feeding difficulty with impaired swallowing was observed in most patients, defective swallowing would have compromised absorption of amniotic fluid. Thus, both body and placental factors are assumed for the development of polyhydramnios. This would explain why polyhydramnios was observed in patients #1, #6, and #8 who were free from placentomegaly, and in patient #22 who showed no feeding difficulty, although the presence of feeding difficulty was unknown for patient #1 as was placentomegaly for patient #22. In addition, since amniotic fluid begins to increase from 8–11 weeks of gestation and reaches its maximum volume around 32 weeks of gestation,[18,19] this would explain why amnioreduction was usually required from 30 weeks of gestation.

Second, birth size was relatively well preserved, whereas postnatal growth was rather compromised. The well preserved prenatal growth in apparently compromised intrauterine environments would be consistent with the conflict theory that overexpression of *PEGs* promotes fetal and placental growth.[20] Notably, birth weight was disproportionately greater than birth length in the apparent absence of generalized edema. In this regard, mouse *Dlk1*, *Rtl1*, and *Gtl2* (*Meg3*) on the distal part of chromosome 12 are expressed in skeletal muscles (Supplementary Figure S5),[14,17] and paternal disomy for chromosome 12 causes muscular hypertrophy.[21] Thus, patients with UPD(14)pat and related conditions may have muscular hypertrophy especially in the fetal life. The compromised postnatal growth would primarily be because of poor nutrition caused by feeding difficulties, whereas relative overweight suggestive of possible muscular hypertrophy remains to be recognized.

Third, DD/ID was invariably present in all 26 patients examined for their developmental/intellectual status, with the median DQ/IQ of 55. In this regard, mouse *Dlk1*, *Rtl1*, and *Gtl2* (*Meg3*) are expressed in the brain during embryogenesis (Supplementary Figure S5),[22] and *Dlk1* is involved in the differentiation of midbrain dopaminergic neurons.[22] Thus, DD/ID would primarily be ascribed to the altered expression dosage of *PEGs/MEGs* in the brain.

Fourth, hepatoblastoma was identified in three patients of UPD-group during infancy. In this context, it has been reported that (1) mouse *Dlk1*, *Rtl1*, and *Meg3* (*Gtl2*) are expressed in the fetal liver, but not in the adult liver; [14,17,23,24] (2) overexpression of *Rtl1* in the adult mouse liver has induced hepatic tumors with high penetrance;[24] (3) *Meg3* functions as a tumor suppressor gene in mice;[25] (4) human *DLK1* is expressed in the hepatocytes of 5–6 weeks old embryos;[26] and (5) human DLK1 protein is upregulated in hepatoblastoma.[27] These findings imply the relevance of excessive *RTL1* expression and loss of *MEG3* expression to the occurrence of hepatoblastoma in UPD(14)pat and related conditions, while it remains to be determined whether the DLK1 upregulation is the cause or the result of hepatoblastoma development. Thus, periodical screening for hepatoblastoma, such as serum α-fetoprotein measurement and abdominal ultrasonography, is recommended. In this context, it remains to be studied whether other embryonal tumors may also be prone to occur in UPD(14)pat and related conditions.

Fifth, mortality was high in Del-group and null in Epi-group. The high mortality in Del-group would primarily be ascribed to the high prevalence of premature delivery, although it is unknown whether the high prevalence of premature delivery is an incidental finding or characteristic of Del-group. The null mortality in Epi-group may be due to possible mosaicism with cells accompanied by a normal expression pattern because of escape from epimutation, as reported previously.[28,29] It is unknown, however, whether possible presence of trisomic cells in TR-mediated UPD(14)pat and that of normal cells in PE-mediated UPD(14) may have exerted clinical effects. Notably, since

death was observed only in patients <4 years of age, the vital prognosis is expected to be good from childhood. In addition, since three patients died during respiratory infections, careful management is recommended during such infections.

Furthermore, the present study also provides several useful clinical implications: (1) two patients had Robertsonian translocations as a risk factor for the development of UPD.[30] Thus, karyotyping is suggested for patients with an UPD(14)pat-like phenotype; (2) prenatal detection of polyhydramnios and thoracic and abdominal features is possible from ~25 weeks of gestation; (3) mechanical ventilation and gastric tube feeding are usually required, with variable durations; (4) there was no patient in UPD-group who exhibited clinical features that are attributable to the unmasking of a recessive mutation(s) of paternal origin; (5) since UPD(14)pat and related conditions share several clinical features including embryonal tumors with BWS (Supplementary Table S4), UPD(14)pat and related conditions may be worth considering in atypical or underlying factor-unknown BWS; and (6) since clinical findings are comparable between patients examined in this study and 17 similarly affected non-Japanese patients (Supplementary Table S5), our data will be applicable to non-Japanese patients as well.

A critical matter for UPD(14)pat and related conditions is the lack of a syndrome name. Although the term 'UPD(14)pat syndrome' has been utilized previously,[4] the term is confusing because 'UPD(14)pat syndrome' can be caused by (epi)genetic mechanisms other than UPD (14)pat. In this regard, the name 'Temple syndrome' has been proposed for UPD(14)mat and related conditions or 'UPD(14)mat syndrome',[31,32] a mirror image of UPD(14)pat and related conditions. On the basis of our previous and present studies that have made a significant contribution to the clarification of underlying (epi)genetic factors and the definition of clinical findings, we would propose the name 'Kagami–Ogata syndrome', or 'Wang–Kagami–Ogata syndrome' with the name of Wang who first described UPD(14)pat,[33] for UPD (14)pat and related conditions.

In summary, although the number of patients still remains small, especially in each subtype of Del-group, the present study reveals pathognomic and characteristic clinical findings in UPD(14)pat and related conditions. Furthermore, this study shows the invariable occurrence of DD/ID and the occasional (8.8%) development of hepatoblastoma, thereby showing the necessity of adequate support for DD/ID and screening of hepatoblastoma in affected patients. Finally, we propose the name 'Kagami–Ogata syndrome' for UPD(14)pat and related conditions.

CONFLICT OF INTEREST

The authors declare no conflict of interest.

ACKNOWLEDGEMENTS

We are grateful to all patients and their parents for their cooperation. We thank Drs Haruhiko Sago, Aiko Sasaki, Jun Shibasaki, Rika Kosaki, Michiko Hayashidani, Toshio Takeuchi, Shinya Tanaka, Mika Noguchi, Goro Sasaki, Kouji Masumoto, Takeshi Utsunomiya, Yumiko Komatsu, Hirofumi Ohashi, Hiroshi Kishimoto, Maureen J O'Sullivan, Andrew J Green, Yoshiyuki Watabe, Tsuyako Iwai, Hitoshi Kawato, Akiko Yamamoto, Nobuhiro Suzumori, Hiroko Ueda, Makoto Kuwajima, Kiyoko Samejima, Hiroshi Yoshihashi, Yoriko Watanabe, Jin Nishimura, Shuku Ishikawa, Michiko Yamanaka, Machiko Nakagawa, Hiroharu Inoue, Takashi Imamura, Keiichi Motoyama and Ryoko Yoshinare for providing us with detailed clinical data and materials for molecular studies, Dr Gen Nishimura for interpretation of roentgengraphic findings, and Drs Tadayuki Ayabe, Keiko Matsubara, Yoichi Sekita and Maki Fukami for their support in molecular analyses. We also thank Ms. Emma Barber for her editorial assistance with the final draft of this paper. This work was supported by Grants-in-Aid for Scientific Research (A) (25253023) and Research (B) (23390083) from the Japan Society for the Promotion of Science (JSPS), and by Grants for Health Research on Children, Youth, and Families (H25-001) and for Research on Intractable Diseases (H22-161) from the Ministry of Health, Labor and Welfare (MHLW), by Grants from the National Center for Child Health and Development (23A-1, 25-10), and by Grant from Takeda Science Foundation.

1 da Rocha ST, Edwards CA, Ito M, Ogata T, Ferguson-Smith AC: Genomic imprinting at the mammalian Dlk1-Dio3 domain. *Trends Genet* 2008; **24**: 306–316.
2 Kagami M, Sekita Y, Nishimura G *et al*: Deletions and epimutations affecting the human 14q32.2 imprinted region in individuals with paternal and maternal upd(14)-like phenotypes. *Nat Genet* 2008; **40**: 237–242.
3 Kagami M, O'Sullivan MJ, Green AJ *et al*: The IG-DMR and the MEG3-DMR at human chromosome 14q32.2: hierarchical interaction and distinct functional properties as imprinting control centers. *PLoS Genet* 2010; **6**: e1000992.
4 Beygo J, Elbracht M, de Groot K *et al*: Novel deletions affecting the MEG3-DMR provide further evidence for a hierarchical regulation of imprinting in 14q32. *Eur J Hum Genet* 2015; **23**: 180–188.
5 Hoffmann K, Heller R: Uniparental disomies 7 and 14. *Best Pract Res Clin Endocrinol Metab* 2011; **25**: 77–100.
6 Kagami M, Matsuoka K, Nagai T *et al*: Paternal uniparental disomy 14 and related disorders: placental gene expression analyses and histological examinations. *Epigenetics* 2012; **7**: 1142–1150.
7 Kurosawa K, Sasaki H, Sato Y *et al*: Paternal UPD14 is responsible for a distinctive malformation complex. *Am J Med Genet* 2002; **110**: 268–272.
8 Kagami M, Nishimura G, Okuyama T *et al*: Segmental and full paternal isodisomy for chromosome 14 in three patients: narrowing the critical region and implication for the clinical features. *Am J Med Genet A* 2005; **138A**: 127–132.
9 Kagami M, Kato F, Matsubara K, Sato T, Nishimura G, Ogata T: Relative frequency of underlying genetic causes for the development of UPD(14)pat-like phenotype. *Eur J Hum Genet* 2012; **20**: 928–932.
10 Horii M, Horiuchi H, Momoeda M, Nakagawa M *et al*: Hepatoblastoma in an infant with paternal uniparental disomy 14. *Congenit Anom (Kyoto)* 2012; **52**: 219–220.
11 Miyazaki O, Nishimura G, Kagami M, Ogata T: Radiological evaluation of dysmorphic thorax of paternal uniparental disomy 14. *Pediatr Radiol* 2011; **41**: 1013–1019.
12 Parveen Z, Tongson-Ignacio JE, Fraser CR, Killeen JL, Thompson KS: Placental mesenchymal dysplasia. *Arch Pathol Lab Med* 2007; **131**: 131–137.
13 Williams DH, Gauthier DW, Maizels M: Prenatal diagnosis of Beckwith–Wiedemann syndrome. *Prenat Diagn* 2005; **25**: 879–884.
14 da Rocha ST, Tevendale M, Knowles E, Takada S, Watkins M, Ferguson-Smith AC: Restricted co-expression of Dlk1 and the reciprocally imprinted non-coding RNA, Gtl2: implications for cis-acting control. *Dev Biol* 2007; **306**: 810–823.
15 da Rocha ST, Charalambous M, Lin SP *et al*: Gene dosage effects of the imprinted delta-like homologue 1 (dlk1/pref1) in development: implications for the evolution of imprinting. *PLoS Genet* 2009; **5**: e1000392.
16 Sekita Y, Wagatsuma H, Nakamura K *et al*: Role of retrotransposon-derived imprinted gene, Rtl1, in the feto-maternal interface of mouse placenta. *Nat Genet* 2008; **40**: 243–248.
17 Brandt J, Schrauth S, Veith AM *et al*: Transposable elements as a source of genetic innovation: expression and evolution of a family of retrotransposon-derived neogenes in mammals. *Gene* 2005; **345**: 101–111.
18 Modena AB, Fieni S: Amniotic fluid dynamics. *Acta Biomed* 2004; **75**: 11–13.
19 Beall MH, van den Wijngaard JP, van Gemert MJ, Ross MG: Amniotic fluid water dynamics. *Placenta* 2007; **28**: 816–823.
20 Hurst LD, McVean GT: Growth effects of uniparental disomies and the conflict theory of genomic imprinting. *Trends Genet* 1997; **13**: 436–443.
21 Georgiades P, Watkins M, Surani MA, Ferguson-Smith AC: Parental origin-specific developmental defects in mice with uniparental disomy for chromosome 12. *Development* 2000; **127**: 4719–4728.
22 Wilkinson LS, Davies W, Isles AR: Genomic imprinting effects on brain development and function. *Nat Rev Neurosci* 2007; **8**: 832–843.
23 Kang ER, Iqbal K, Tran DA *et al*: Effects of endocrine disruptors on imprinted gene expression in the mouse embryo. *Epigenetics* 2011; **6**: 937–950.
24 Riordan JD, Keng VW, Tschida BR *et al*: Identification of rtl1, a retrotransposon-derived imprinted gene, as a novel driver of hepatocarcinogenesis. *PLoS Genet* 2013; **9**: e1003441.
25 Zhou Y, Zhang X, Klibanski A: MEG3 noncoding RNA: a tumor suppressor. *J Mol Endocrinol* 2012; **48**: R45–R53.
26 Floridon C, Jensen CH, Thorsen P *et al*: Does fetal antigen 1 (FA1) identify cells with regenerative, endocrine and neuroendocrine potentials? A study of FA1 in embryonic, fetal, and placental tissue and in maternal circulation. *Differentiation* 2000; **66**: 49–59.
27 Falix FA, Aronson DC, Lamers WH, Hiralall JK, Seppen J: DLK1, a serum marker for hepatoblastoma in young infants. *Pediatr Blood Cancer* 2012; **59**: 743–745.
28 Yamazawa K, Kagami M, Fukami M, Matsubara K, Ogata T: Monozygotic female twins discordant for Silver-Russell syndrome and hypomethylation of the H19-DMR. *J Hum Genet* 2008; **53**: 950–955.